

A semi-classical field method for the equilibrium Bose gas and application to thermal vortices in two dimensions

Luca Giorgetti,¹ Iacopo Carusotto,¹ and Yvan Castin²

¹*CNR-BEC-INFM and Dipartimento di Fisica, Università di Trento, I-38050 Povo, Italy*

²*Laboratoire Kastler Brossel, Ecole normale supérieure, UPMC,
CNRS, 24 rue Lhomond, F-75231 Paris Cedex 5, France*

(Dated: January 6, 2022)

We develop a semi-classical field method for the study of the weakly interacting Bose gas at finite temperature, which, contrarily to the usual classical field model, does not suffer from an ultraviolet cut-off dependence. We apply the method to the study of thermal vortices in spatially homogeneous, two-dimensional systems. We present numerical results for the vortex density and the vortex pair distribution function. Insight in the physics of the system is obtained by comparing the numerical results with the predictions of simple analytical models. In particular, we calculate the activation energy required to form a vortex pair at low temperature.

PACS numbers: 02.70.Ss 03.75.Lm 67.40.Vs

I. INTRODUCTION

Classical field theories are a widespread and flexible tool for the study of many aspects of the physics of ultracold Bose gases. Developed in particular to address time-dependent problems related to dynamical aspects of the Bose-Einstein phase transition [1, 2] they can also be used to study thermal equilibrium properties of the weakly interacting Bose gas [3, 4]. A major example is the quantitative prediction of the shift of the Bose-Einstein condensation temperature due to atomic interactions [5] that has been obtained by means of a Monte Carlo sampling of a classical field model [6]: as long as the physics of the system is determined by the low-energy modes, classical field models provide reliable results on the full quantum problem. Classical field techniques have also been applied to obtain analytical and numerical predictions for reduced dimensionality Bose systems [4, 7, 8, 9], including the calculation of the critical temperature for the Berezinskii-Kosterlitz-Thouless transition in two dimensions [10, 11]. However, an ultraviolet cut-off has to be introduced in most of these classical field techniques in order to avoid ultraviolet divergences analogous to the blackbody catastrophe of classical statistical mechanics, and this raises the problem of a possible cut-off dependence of some of the physical results.

On the other side, several exact reformulations of the many boson problem have been developed. Although they have successfully served as a starting point for Quantum Monte Carlo simulations [12, 13] of the thermal properties of Bose systems such as liquid Helium and ultracold atomic gases [14, 15, 16], they often lack the intuitiveness of classical field theories where the physics is described in terms of a simple distribution function in the functional space of c -number fields.

The present paper is devoted to the development, the validation, and the first application of a *semi*-classical field theory which tries to combine a regular behavior in the ultraviolet limit with a transparent intuition of the

physics of the system. As in classical field theories, the density matrix of the Bose system is written in terms of a distribution in the space of c -number fields. In the semi-classical theory, this distribution is however much more complex than a simple Boltzmann factor $\exp(-E/k_B T)$, where E would be the Gross-Pitaevskii energy of the field configuration, and has to be obtained as the result of an imaginary-time Gross-Pitaevskii evolution starting from an initially uniform distribution in functional space.

A first application of the method is then presented to the study of thermal vortices in a homogeneous two-dimensional Bose gas, in particular their density and their pair distribution function. Experimentally, the two-dimensional Bose gas has been realized some time ago [17, 18], but it is only recently that several experiments have given indications of the presence of vortices in finite temperature samples [19, 20, 21], and this raises the question of the link between observable quantities (e.g the vortex density), and theoretical concepts such as the Berezinskii-Kosterlitz-Thouless (BKT) transition [10, 11, 22, 23, 24]. Most of the existing theoretical treatments neglect all density fluctuations other than the ones in the vicinity of a vortex core, and eventually map the 2D Bose gas problem onto the XY model of statistical mechanics [25]. Although this approximation is expected to provide a good description of atomic gases trapped in 2D optical lattices [21, 26, 27], it seems far from being accurate for spatially continuous systems: at temperatures of the order of the BKT transition temperature, the amplitude of the density fluctuations in the gas is not negligible as compared to the density itself [28]. Our work aims at going beyond this approximation so to fully include the effect of density fluctuations. The fact that it is based on c -number fields gives to the present semi-classical method an advantage over standard Quantum Monte Carlo techniques in view of the study of vortices.

The paper is divided in two main parts. In the first part (Sec.II), we introduce the semi-classical method in the grand-canonical (Sec.II A) and in the canonical (Sec.II C) ensembles, and we characterize its range of

applicability (Sec.II B). In the second part (Sec.III), we discuss the physics of the two-dimensional Bose gas. The numerical results are presented in Sec.III A: different observables are considered, e.g. the normal and non-condensed fractions, the density fluctuations, the vortex density, and the vortex pair-distribution function. In Sec.III B the effect of Bose condensation on the vortex density in the finite size ideal gas is discussed analytically; this requires the use of the canonical ensemble, which introduces new features with respect to the well-studied grand canonical case [29, 30]. In Sec.III C a simple model including the interacting case is developed to understand the numerical results, principally the ones for the vortex density $n_{v,+}$: an activation law of the form $n_{v,+} \propto \exp(-\Delta/k_B T)$ is found in the low-temperature regime, and the dependence of $\Delta(T)$ on the system parameters such as the interaction strength and the system size is discussed: the main qualitative differences between the ideal and the interacting gas behaviors are pointed out. Conclusions are finally drawn in Sec.IV.

II. THE SEMI-CLASSICAL METHOD

A. In the grand-canonical ensemble

Consider a Bose field defined on an square lattice of \mathcal{N} points with periodic boundary conditions; V is the total volume of the quantization box and $dV = V/\mathcal{N}$ is the volume of the unit cell of the lattice. The Bose field operators $\hat{\Psi}(\mathbf{r})$ obey the Bose commutation relations $[\hat{\Psi}(\mathbf{r}), \hat{\Psi}^\dagger(\mathbf{r}')] = \delta_{\mathbf{r},\mathbf{r}'}/dV$.

The state of the Bose field is described by the density operator ρ , which can be expanded in the so-called Glauber-P representation on coherent states:

$$\rho = \int \mathcal{D}\psi P[\psi] |\text{coh} : \psi\rangle \langle \text{coh} : \psi|, \quad (1)$$

where $P[\psi]$, the Glauber-P distribution, is guaranteed to exist in the sense of distributions but in general is not a positive nor even a regular function [31, 32, 33]. $\psi(\mathbf{r})$ is here a c-number field defined on the lattice, the coherent state is defined as usual as:

$$|\text{coh} : \psi\rangle = \exp\left[-\frac{1}{2}\|\psi\|^2\right] \exp\left\{\sum_{\mathbf{r}} dV \psi(\mathbf{r}) \hat{\Psi}^\dagger(\mathbf{r})\right\} |0\rangle, \quad (2)$$

where $\|\psi\|^2 = dV \sum_{\mathbf{r}} |\psi(\mathbf{r})|^2$, and the functional integration is performed over the value of the complex field at each of the \mathcal{N} sites of the lattice:

$$\mathcal{D}\psi = \prod_{\mathbf{r}} d\text{Re}[\psi(\mathbf{r})] d\text{Im}[\psi(\mathbf{r})]. \quad (3)$$

The homogeneous Bose gas is described by the follow-

ing second-quantized Hamiltonian:

$$\mathcal{H} = \sum_{\mathbf{k}} \left[\frac{\hbar^2 k^2}{2m} - \mu \right] \hat{a}_{\mathbf{k}}^\dagger \hat{a}_{\mathbf{k}} + \frac{g_0}{2} \sum_{\mathbf{r}} dV \hat{\Psi}^\dagger(\mathbf{r}) \hat{\Psi}^\dagger(\mathbf{r}) \hat{\Psi}(\mathbf{r}) \hat{\Psi}(\mathbf{r}). \quad (4)$$

The single-particle dispersion relation within the first Brillouin zone is taken as parabolic with mass m , μ is the chemical potential, and the interactions are modeled by a two-body discrete delta potential of strength g_0 .

The gas is assumed to be at thermal equilibrium at a temperature T , so that the unnormalized density operator is $\rho_{\text{eq}}(\beta) = \exp[-\beta \mathcal{H}]$ with $\beta = 1/k_B T$. This density operator can be obtained as the result of an imaginary-time evolution:

$$\frac{d\rho_{\text{eq}}}{d\tau} = -\frac{1}{2} \{\mathcal{H}, \rho_{\text{eq}}\} = -\frac{1}{2} [\mathcal{H}\rho_{\text{eq}} + \rho_{\text{eq}}\mathcal{H}] \quad (5)$$

during the ‘‘time’’ interval $\tau = 0 \rightarrow \beta$, starting from the identity operator $\rho_{\text{eq}}(\tau = 0) = \mathbf{1}$.

In the Glauber-P representation, the imaginary-time evolution takes the form of a Fokker-Planck-like partial differential equation:

$$\partial_\tau P[\psi] = -E[\psi] P[\psi] - \sum_{\mathbf{r}} \left[\partial_{\psi(\mathbf{r})} (F[\psi] P[\psi]) + \frac{g_0}{4dV} \partial_{\psi(\mathbf{r})}^2 (\psi^2(\mathbf{r}) P[\psi]) + \text{c.c.} \right] \quad (6)$$

for the distribution function $P[\psi]$ in the phase-space of the c-number fields defined on the lattice. The derivatives with respect to the complex field $\psi(\mathbf{r})$ are defined as usual as:

$$\partial_{\psi(\mathbf{r})} = \frac{1}{2} [\partial_{\text{Re}[\psi(\mathbf{r})]} - i\partial_{\text{Im}[\psi(\mathbf{r})]}]. \quad (7)$$

The first term in the right-hand side of (6) acts on the weight of the wavefunction ψ and involves the mean-field energy of the complex field $\psi(\mathbf{r})$:

$$E[\psi] = \sum_{\mathbf{r}} dV \psi^*(\mathbf{r}) [h_0 - \mu] \psi(\mathbf{r}) + \frac{g_0}{2} \sum_{\mathbf{r}} dV |\psi(\mathbf{r})|^4. \quad (8)$$

h_0 is a shorthand for the single-particle Hamiltonian, whose k -space form is $h_0 = \hbar^2 k^2 / (2m)$.

The second term is a drift term consisting of the imaginary-time Gross-Pitaevskii evolution:

$$F[\psi](\mathbf{r}) = -\frac{1}{2dV} \partial_{\psi^*(\mathbf{r})} E[\psi] = -\frac{1}{2} [h_0 - \mu + g_0 |\psi(\mathbf{r})|^2] \psi(\mathbf{r}). \quad (9)$$

Finally, the diffusion terms involving the second-order derivatives are local in space, but have a non-positive-definite diffusion matrix:

$$D(\mathbf{r}) = -\frac{g_0}{4dV} \begin{pmatrix} 0 & \psi^2(\mathbf{r}) \\ \psi^{*2}(\mathbf{r}) & 0 \end{pmatrix}. \quad (10)$$

A complete solution of the partial differential equation (6) would provide the exact result of the lattice quantum field problem defined by the Hamiltonian (4). Unfortunately, the non-positive-definite nature of the diffusion matrix (10) prevents the Fokker-Planck-like equation (6) from being directly mappable on a stochastic field problem for ψ . Some approximation schemes are therefore required in order to perform numerical simulations within the Glauber-P framework.

In our previous work [8], the high-temperature physics of the one-dimensional Bose gas was studied by keeping only the first term in the right-hand side of (6). The resulting distribution in the phase-space of the c-number fields is the usual Boltzmann one $P[\psi] = \exp(-E[\psi]/k_B T)$ in terms of the mean-field energy (8). A better approximation is obtained by keeping also the drift force (9) and neglecting the diffusion term (10) only. In this case, the partial differential equation (6) can be mapped onto a deterministic evolution for the field $\psi(\mathbf{r})$ and a weight \mathcal{W} :

$$\partial_\tau \psi(\mathbf{r}, \tau) = -\frac{1}{2}[h_0 - \mu + g_0 |\psi(\mathbf{r}, \tau)|^2] \psi(\mathbf{r}, \tau), \quad (11)$$

$$\partial_\tau \mathcal{W}(\tau) = -E[\psi(\tau)] \mathcal{W}(\tau). \quad (12)$$

Physical quantities are then obtained as averages over the initial values for ψ . A possible representation of the initial state $\rho_{\text{eq}}(\tau = 0) = \mathbf{1}$ is to take the initial value of the field $\psi(\mathbf{r}, \tau = 0)$ at each lattice point as uniformly distributed in the complex space and to take a constant initial weight $\mathcal{W}(\tau = 0) = w_0$. This leads to the *semi-classical* approximation for the density operator at temperature T :

$$\rho_{\text{SC}} = \int \mathcal{D}\psi(0) \mathcal{W}(\beta) |\text{coh} : \psi(\beta)\rangle \langle \text{coh} : \psi(\beta)|, \quad (13)$$

where both $\mathcal{W}(\beta)$ and $\psi(\beta)$ depend on the initial value of the field $\psi(0)$.

As the diffusion term (10) is proportional to the interaction strength g_0 , the semi-classical approximation becomes exact in the case of the free Bose field, i.e. for an ideal Bose gas. As a consequence, it does not suffer from the typical ultraviolet divergences of classical field theories, even in presence of interactions.

B. Limits of validity

In order to validate the semi-classical approximation and appreciate its power and its limits, it is interesting to apply it to the simple case of the Bogoliubov Hamiltonian

$$\mathcal{H}_{\text{Bog}} = \sum_{\mathbf{k} \neq 0} \left(\frac{\hbar^2 k^2}{2m} + \mu \right) \hat{a}_{\mathbf{k}}^\dagger \hat{a}_{\mathbf{k}} + \frac{\mu}{2} \left(\hat{a}_{\mathbf{k}}^\dagger \hat{a}_{-\mathbf{k}}^\dagger + \hat{a}_{\mathbf{k}} \hat{a}_{-\mathbf{k}} \right). \quad (14)$$

This Hamiltonian being quadratic in the field operators, the semi-classical equations (11-12) can be analytically

solved and their prediction compared to the exact quantum results.

By defining the operators $\hat{c}_{\mathbf{k},+} = (\hat{a}_{\mathbf{k}} + \hat{a}_{-\mathbf{k}})/\sqrt{2}$ and $\hat{c}_{\mathbf{k},-} = (\hat{a}_{\mathbf{k}} - \hat{a}_{-\mathbf{k}})/(i\sqrt{2})$, the Bogoliubov Hamiltonian (14) can be rewritten as a sum of terms involving independent \mathbf{k} modes:

$$\mathcal{H}_{\text{Bog}} = \sum'_{\mathbf{k}, \epsilon = \pm} \mathcal{H}_{\mathbf{k}, \epsilon} = \sum'_{\mathbf{k}, \epsilon = \pm} \left(\frac{\hbar^2 k^2}{2m} + \mu \right) \hat{c}_{\mathbf{k}, \epsilon}^\dagger \hat{c}_{\mathbf{k}, \epsilon} + \frac{\mu}{2} \left(\hat{c}_{\mathbf{k}, \epsilon}^\dagger \hat{c}_{\mathbf{k}, \epsilon}^\dagger + \hat{c}_{\mathbf{k}, \epsilon} \hat{c}_{\mathbf{k}, \epsilon} \right). \quad (15)$$

In this way, the Glauber-P distribution factorises as a product of independent factors involving the different \mathbf{k} modes. To avoid double-counting of modes, the primed sum is restricted to those \mathbf{k} vectors which are contained in an (arbitrarily chosen) half-space.

Each term of the Hamiltonian (15) has the simple structure of a one-mode squeezing Hamiltonian:

$$\mathcal{H}_1 = (E_k + \mu) \hat{c}^\dagger \hat{c} + \frac{\mu}{2} (\hat{c}^2 + \hat{c}^{\dagger 2}), \quad (16)$$

with the kinetic energy coefficient $E_k = \hbar^2 k^2/(2m)$ and the \hat{c} operator corresponding to any of $\hat{c}_{\mathbf{k}, \pm}$ in (15).

Since the Hamiltonian (16) is quadratic, the exact Glauber-P distribution for the thermal equilibrium state can be analytically obtained by means of standard techniques [33], as well as its semi-classical approximation: as shown in the Appendix A, both distributions have a Gaussian form,

$$P(\gamma) \propto e^{-(\text{Re } \gamma)^2/\sigma_R^2} e^{-(\text{Im } \gamma)^2/\sigma_I^2}. \quad (17)$$

The widths for the exact distribution are given by

$$(\sigma_R^2)_{\text{ex}} = \frac{1}{2} \left[\left(\frac{E_k}{E_k + 2\mu} \right)^{1/2} \coth \left(\frac{\beta \epsilon_k}{2} \right) - 1 \right] \quad (18)$$

$$(\sigma_I^2)_{\text{ex}} = \frac{1}{2} \left[\left(\frac{E_k + 2\mu}{E_k} \right)^{1/2} \coth \left(\frac{\beta \epsilon_k}{2} \right) - 1 \right] \quad (19)$$

where $\epsilon_k = [E_k(2\mu + E_k)]^{1/2}$ is the energy of the Bogoliubov mode. When the temperature is too low, $(\sigma_R^2)_{\text{ex}}$ becomes negative, so that the Glauber-P distribution ceases to exist as a regular function [32, 33]. The corresponding lower bound on the temperature is plotted in Fig.1. Two limiting cases are easily isolated: for low-energy modes such that $E_k \rightarrow 0$, the positivity condition for the Glauber-P distribution is the simple one $k_B T > \mu$. For high energy modes, the condition is instead more stringent, $k_B T > (E_k + \mu)/|\log(\mu/2E_k)|$.

The widths for the semi-classical approximation are given by

$$(\sigma_R^2)_{\text{SC}} = \left[e^{\beta(E_k + 2\mu)} - 1 \right]^{-1} \quad (20)$$

$$(\sigma_I^2)_{\text{SC}} = \left[e^{\beta E_k} - 1 \right]^{-1}. \quad (21)$$

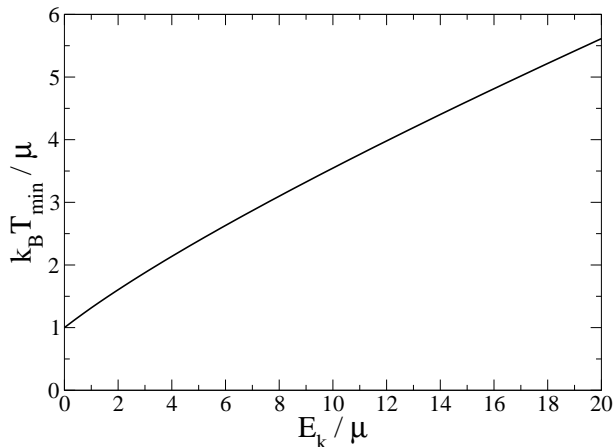


FIG. 1: In the Bogoliubov model, minimal value of the temperature T_{\min} ensuring regularity and positivity of the Glauber-P distribution in a mode \mathbf{k} , as a function of the kinetic energy coefficient E_k of the mode.

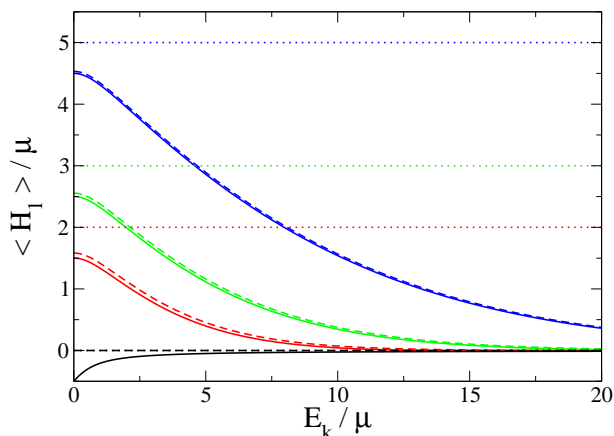


FIG. 2: (Color online) In the Bogoliubov model, mean energy in a mode as a function of the mode kinetic energy coefficient E_k for different values of the temperature $k_B T / \mu = 0, 2, 3, 5$ (from bottom to top). Solid lines: quantum result. Dashed lines: semi-classical theory. Dotted lines: classical field approximation.

As expected, they remain positive at all temperature.

These results are the starting point for detailed comparison of the semi-classical predictions to the exact quantum results for the most significant observables. Let us start with the *mean energy*. The semi-classical value is:

$$\langle \mathcal{H}_1 \rangle_{SC} = \frac{1}{2} \left[\frac{E_k + 2\mu}{e^{\beta(E_k + 2\mu)} - 1} + \frac{E_k}{e^{\beta E_k} - 1} \right], \quad (22)$$

which is to be compared to the exact value

$$\langle \mathcal{H}_1 \rangle_{\text{ex}} = \frac{\epsilon_k}{e^{\beta \epsilon_k} - 1} + \frac{\epsilon_k - (E_k + \mu)}{2}. \quad (23)$$

An order by order comparison can be performed in the high-temperature limit by expanding (22) and (23) in

powers of β :

$$\langle \mathcal{H}_1 \rangle_{SC} \simeq k_B T - \frac{E_k + \mu}{2} + O[\beta(E_k + 2\mu)^2] \quad (24)$$

$$\langle \mathcal{H}_1 \rangle_{\text{ex}} \simeq k_B T - \frac{E_k + \mu}{2} + O(\beta \epsilon_k^2). \quad (25)$$

Agreement is found not only on the classical term $k_B T$, but also on the subleading constant term $-(E_k + \mu)/2$, which would instead be missed by a simple classical field theory.

A more detailed comparison is obtained by working out two limiting regions. In the low energy limit, one has

$$\lim_{\epsilon_k \rightarrow 0} \langle \mathcal{H}_1 \rangle_{\text{ex}} = k_B T - \frac{\mu}{2} \quad (26)$$

$$\lim_{\epsilon_k \rightarrow 0} \langle \mathcal{H}_1 \rangle_{SC} = k_B T - \frac{\mu}{2} + \frac{1}{6} \beta \mu^2 + O(\beta^3 \mu^4) : \quad (27)$$

the relative error of the semi-classical result is therefore of the order of $(\beta \mu)^2/6$, i.e. very small provided $k_B T \gg \mu$.

In the high energy limit $\epsilon_k \rightarrow \infty$, one has instead [34]

$$\langle \mathcal{H}_1 \rangle_{SC} \sim \cosh(\beta \mu) \epsilon_k e^{-\beta \epsilon_k}. \quad (28)$$

In the high temperature regime where $\cosh(\beta \mu) \simeq 1$, this semi-classical prediction almost coincides with the exact value (23) once the zero-point energy is subtracted from the quantum value. This shows that the semi-classical theory does not suffer from any ultraviolet divergence coming from the zero-point energy, nor from the typical black-body catastrophe of classical field theories.

In summary, the semi-classical theory is able to accurately reproduce the value of the average energy under the assumption that the temperature is higher than the chemical potential, $k_B T \gg \mu$. Examples of plots of the mean energy of the different Bogoliubov modes as a function of E_k are presented in Fig.2 for the semi-classical theory, the classical field approximation, and the exact result. The agreement of the semi-classical theory with the exact result is already remarkable for temperatures only a few times higher than the chemical potential, while the classical field approximation is quite crude in predicting a constant mean energy $k_B T$ independent of the mode energy.

Another observable that we consider is the *normal fraction* f_n , defined as

$$f_n = \frac{\langle P_x^2 \rangle}{N m k_B T}, \quad (29)$$

where P_x is the x component of the total momentum of the system. This quantity f_n estimates the response of the Bose system to a gauge field, e.g. a magnetic field in the case of charged particles, or a rotation in the case of neutral ones [35, 36].

The exact quantum result of the Bogoliubov theory [37] has the form

$$\langle P_x^2 \rangle_{\text{ex}} = \sum_{\mathbf{k} \neq 0} \hbar^2 k_x^2 n_{\mathbf{k}} (n_{\mathbf{k}} + 1) \quad (30)$$

where $n_k = (e^{\beta\epsilon_k} - 1)^{-1}$ is the quantum mean occupation number of the Bogoliubov mode. The semi-classical approximation is instead given by

$$\langle P_x^2 \rangle_{SC} = \sum_{\mathbf{k} \neq 0} \hbar^2 k_x^2 \left[(\sigma_R^2)_{SC} (\sigma_I^2)_{SC} + \frac{1}{2} (\sigma_R^2)_{SC} + \frac{1}{2} (\sigma_I^2)_{SC} \right]. \quad (31)$$

It is interesting to compare the expression between square brackets to the quantum value $n_k(n_k + 1)$, at least in the high temperature regime $k_B T \gg \mu$. For low momenta such that $E_k \leq \mu$, the semi-classical approximation correctly reproduces the leading term $(k_B T / \epsilon_k)^2$ and has an error $O(1)$. The relative error is therefore of second order in T . For high momenta $\mu \ll E_k \simeq k_B T$, the semi-classical approximation reproduces the quantum term with a relative error $O[(\beta\mu)^2]$. After summation over all \mathbf{k} states, one finds for a two-dimensional Bogoliubov gas in the thermodynamic limit that both the quantum and the semi-classical values of f_n have the form:

$$f_n = \frac{1}{2\pi n \xi^2} \left\{ \left[1 + \ln \left(\frac{k_B T}{2\mu} \right) \right] \frac{k_B T}{\mu} + \frac{1}{2} + O[\beta\mu \ln(\beta\mu)] \right\}, \quad (32)$$

where ξ is the healing length defined by $\hbar^2 / m \xi^2 = \mu$. These results are summarized in Fig.3, where the semi-classical approximation for f_n is compared to the quantum value as a function of $k_B T / \mu$.

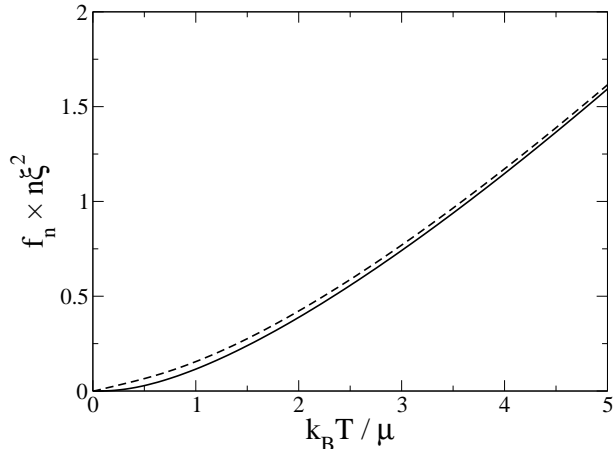


FIG. 3: For a two-dimensional Bogoliubov gas in the thermodynamic limit, normal fraction f_n as a function of the temperature $k_B T$. Solid line: quantum prediction. Dashed line: semi-classical prediction. In order to have (within Bogoliubov theory) a universal function of $k_B T / \mu$, we actually plot the product of f_n times $n \xi^2$, the healing length ξ being defined by $\hbar^2 / m \xi^2 = \mu$.

The last observable that we investigate is the *pair dis-*

tribution function,

$$g^{(2)}(\mathbf{r}' - \mathbf{r}) = \frac{1}{n^2} \left\langle \hat{\Psi}^\dagger(\mathbf{r}) \hat{\Psi}^\dagger(\mathbf{r}') \hat{\Psi}(\mathbf{r}') \hat{\Psi}(\mathbf{r}) \right\rangle. \quad (33)$$

Within the Bogoliubov approximation, this can be written for a two-dimensional system in the thermodynamic limit as:

$$g^{(2)}(\mathbf{r}) \simeq 1 + \frac{2}{n} \int \frac{d^2 \mathbf{k}}{(2\pi)^2} \cos(\mathbf{k} \cdot \mathbf{r}) \left[\langle a_{\mathbf{k}}^\dagger a_{\mathbf{k}} + a_{\mathbf{k}} a_{-\mathbf{k}} \rangle \right] \quad (34)$$

where n is the total density. For a given k , the expectation value between square brackets in (34) is equal to σ_R^2 . Its value is given by Eq.(18) for the quantum theory and by Eq.(20) for the semi-classical theory.

In Fig.4 we plot the pair distribution $g^{(2)}(r)$ as a function of r for various values of the temperature. The narrow dip which appears in the result of the quantum calculation originates from the zero-point fluctuations of the Bogoliubov modes, and is therefore absent in the semi-classical approximation: in the quantum case, the decay of the Fourier transform of $g^{(2)}(\mathbf{r}) - 1$ at large k is in fact algebraic, whereas it is Gaussian in the semi-classical approximation. On the other hand, the semi-classical approximation reproduces remarkably well the intermediate to long-distance behavior already at temperatures as low as $k_B T = 2\mu$.

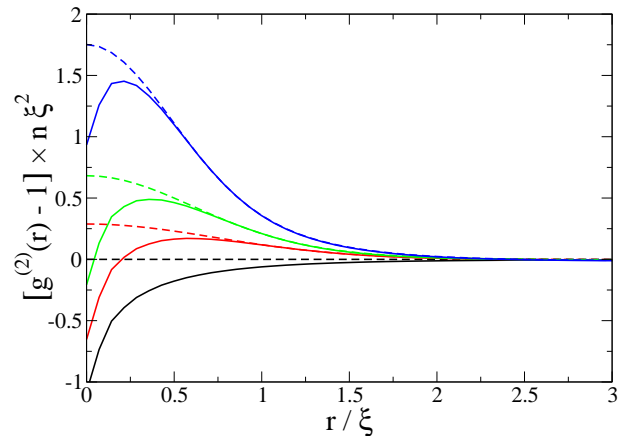


FIG. 4: (Color online) For a two-dimensional lattice Bogoliubov gas in the thermodynamic limit, pair distribution $g^{(2)}(\mathbf{r})$ as a function of r for different values of the temperature, $k_B T / \mu = 0, 2, 3, 5$ (from bottom to top). Solid line: quantum result. Dashed line: semi-classical approximation. In the plot, the product of $g^{(2)} - 1$ with $n \xi^2$ is actually plotted, where n is the density, and ξ the healing length such that $\hbar^2 / (m \xi^2) = \mu$. For the Bogoliubov gas, this product is indeed a universal function of $k_B T / \mu$ and r / ξ . Here the lattice spacing is 0.07ξ .

C. In the canonical ensemble

In the language of [39], the semi-classical method discussed in the previous sections can be seen as a “simple

coherent” scheme from which the noise terms have been dropped. This suggests that a similar procedure may be applied to the “simple Fock” scheme in order to devise a semi-classical method that works in the canonical ensemble, i.e. at a fixed number N of particles.

The building block of this scheme is the Fock state defined as usual as:

$$|N : \psi\rangle = \frac{1}{\sqrt{N!}} (\hat{a}_\psi^\dagger)^N |0\rangle, \quad (35)$$

$|0\rangle$ is here the vacuum state and the \hat{a}_ψ^\dagger operator creates a particle in the (not necessarily normalized) ψ state:

$$\hat{a}_\psi^\dagger = \sum_{\mathbf{r}} dV \psi(\mathbf{r}) \hat{\Psi}^\dagger(\mathbf{r}). \quad (36)$$

By projecting both sides of (1) onto the subspace with exactly N particles, it is easy to see that any N -body density operator can be expanded on a family of Fock states as:

$$\rho = \int_{\|\psi\|=1} \mathcal{D}\psi \mathcal{P}[\psi] |N : \psi\rangle \langle N : \psi|, \quad (37)$$

where the distribution \mathcal{P} is the Fock state equivalent of the Glauber-P distribution, and the integral is taken over the unit sphere $\|\psi\| = 1$. The infinite temperature state $\rho_{\text{eq}}(\tau = 0) = \mathbf{1}$ is obtained by simply taking a constant value for $\mathcal{P}[\psi]$. This corresponds to a random selection of the wavefunction $\psi(\tau = 0)$ with a uniform distribution on the unit sphere $\|\psi\| = 1$. At finite temperature, the distribution function $\mathcal{P}[\psi]$ for an interacting gas is unfortunately not necessarily regular and positive; as a consequence, no stochastic evolution for ψ exists such that the thermal density operator $\rho(\beta)$ is obtained as the average of dyadics of the form $|N : \psi\rangle \langle N : \psi|$. On the other hand, one can find a stochastic evolution ensuring that $\rho(\beta)$ is the average of dyadics of the slightly different form $|N : \psi_1\rangle \langle N : \psi_2|$. ψ_1 and ψ_2 are here independent realizations of the Ito stochastic process [39]

$$d\psi(\mathbf{r}) = -\frac{d\tau}{2} \left[h_0 + g_0 \frac{N-1}{\|\psi\|^2} |\psi(\mathbf{r})|^2 - g_0 \frac{N-1}{2} \frac{\sum_{\mathbf{r}'} dV |\psi(\mathbf{r}')|^4}{\|\psi\|^4} \right] \psi(\mathbf{r}) + dB(\mathbf{r}), \quad (38)$$

starting from the common value $\psi(\tau = 0)$, and the correlation functions of the noise $dB(\mathbf{r})$ satisfy the condition:

$$dB(\mathbf{r}) dB(\mathbf{r}') = -\frac{g_0 d\tau}{2dV} \mathcal{Q}_{\mathbf{r}} \mathcal{Q}_{\mathbf{r}'} [\delta_{\mathbf{r},\mathbf{r}'} \psi(\mathbf{r}) \psi(\mathbf{r}')], \quad (39)$$

where the projector \mathcal{Q} projects orthogonally to the ket $|\psi\rangle$.

From this exact reformulation of the full many-body problem, it is immediate to obtain a canonical version of the semi-classical scheme by simply neglecting the noise term dB in (38). Intuitively this is expected to constitute

a good approximation of the quantum model at least in the high-temperature case, i.e. for ‘times’ τ short enough for the effect of the noise terms to remain small. The corresponding semi-classical approximation of the density operator for the thermal equilibrium state at temperature T in the canonical ensemble is therefore

$$\rho_{\text{SC}} = \int_{\|\psi(0)\|=1} \mathcal{D}\psi(0) |N : \psi(\beta)\rangle \langle N : \psi(\beta)|, \quad (40)$$

where $\psi(\beta)$ has evolved from its initial value $\psi(0)$ during a ‘time’ β according to the deterministic part of (38),

$$\partial_\tau \psi(\mathbf{r}, \tau) = -\frac{1}{2} \left[h_0 + g_0 \frac{N-1}{\|\psi\|^2} |\psi(\mathbf{r}, \tau)|^2 - g_0 \frac{N-1}{2} \frac{\sum_{\mathbf{r}'} dV |\psi(\mathbf{r}', \tau)|^4}{\|\psi\|^4} \right] \psi(\mathbf{r}, \tau), \quad (41)$$

which closely resembles an imaginary time Gross-Pitaevskii equation.

This semi-classical Fock scheme can be used as the core of a numerical Monte Carlo code to study the properties of a N -body Bose gas at thermal equilibrium. From the computational point of view, the only non trivial aspect is how to efficiently perform the sampling of $\psi(0)$ on the unit sphere. The numerical algorithm that we have adopted for this purpose is detailed in the appendix B.

III. APPLICATION TO THERMAL VORTICES IN THE 2D GAS

In this second part of the paper, we apply the semi-classical technique developed in the first part to the study of some among the most significant properties of a homogeneous two-dimensional Bose gas at thermal equilibrium in the canonical ensemble. This problem of the 2D Bose gas is under active experimental investigation. It is known theoretically that the 2D Bose gas exhibits the Berezinskii-Kosterlitz-Thouless transition [22, 23, 24], and this transition was recently observed with cold atoms in [20]. An interesting aspect of the experiments with atoms is that they have access to vortices [20, 21], so that special attention will be paid here to observables such as the density and the pair distribution function of thermally activated vortices, for which classical field methods [9] and in particular the present semi-classical field method, are well suited. Our numerical results will then be interpreted in terms of simplified analytical models, which allow one to unravel the underlying physics.

The model Hamiltonian used to describe the system is the two-dimensional version of the spatially homogeneous lattice model (4) with periodic boundary conditions. The value of the coupling constant g_0 to be used in the calculations depends on the details of the atomic confinement along the third dimension: here, we assume a harmonic confinement in the z direction, with a harmonic oscillator length $a_{\text{ho}} = \sqrt{\hbar/m\omega_z}$ much larger than the three-dimensional s -wave scattering length $a_{3\text{D}}$. In this limit,

one is allowed to neglect the energy-dependence of the effective two-dimensional coupling constant g [40, 41], and to simply take [42]

$$g_0 = \frac{\hbar^2}{m} \frac{2\sqrt{2\pi}a_{3D}}{a_{ho}}. \quad (42)$$

To ensure the two dimensional character of the atomic gas, we assume that both the thermal energy $k_B T$ and the mean field zero-temperature chemical potential $g_0 n$ are much smaller than the confinement energy $\hbar\omega_z$ in the z direction. Note that the semi-classical approach is limited to the weakly interacting gas regime $n\xi^2 \gg 1$, the healing length ξ being defined by $\hbar^2/m\xi^2 = ng_0$. Remarkably, this condition reduces to the density-independent one $mg_0/\hbar^2 \ll 1$ in two dimensions.

A. Numerical results

1. Normal and non-condensed fractions

The normal fraction (29) describes the response of the fluid to a spatial twist of the phase [35, 36], while the non-condensed fraction is simply the fraction of atoms in single-particle states other than the zero-momentum plane wave $f_{nc} = 1 - N_0/N$. These two quantities are plotted in Fig.5 as functions of the temperature for three different values of the interaction strength g_0 , including the ideal gas $g_0 = 0$. The overall behavior is almost the same for all the curves: the dependence on temperature is always smooth and, as expected, both the normal and the non-condensed fractions tend to 1 (0) in respectively the high (low) temperature limit. However, whereas the shape of the curve giving the non-condensed fraction is not qualitatively modified as g_0 grows, the crossover from 0 to 1 of the normal fraction turns out to become somehow sharper as the interaction strength is increased [43].

It is interesting to compare the results for the ideal gas case with a (trivial) calculation performed in the grand canonical ensemble: as one can see in Fig.5a, the dashed line corresponding to the grand canonical prediction significantly deviates from the numerical simulation results. A simple explanation for this can be put forward in terms of the finite size of the system, which can indeed lead to differences between the two ensembles. In particular for a Bose condensed ideal gas, the grand canonical ensemble predicts unphysically large fluctuations of the number of condensate particles [45, 46, 47]; although this does not significantly affect the normal and the non-condensed fractions plotted here, it will have a dramatic impact on other quantities like the density fluctuations and the mean vortex density that will be studied in what follows.

In order to fully clarify this issue, an exact canonical calculation can be performed by means of the standard canonization procedure [48]: the analytical predictions for the normal and the non-condensed fractions are plot-

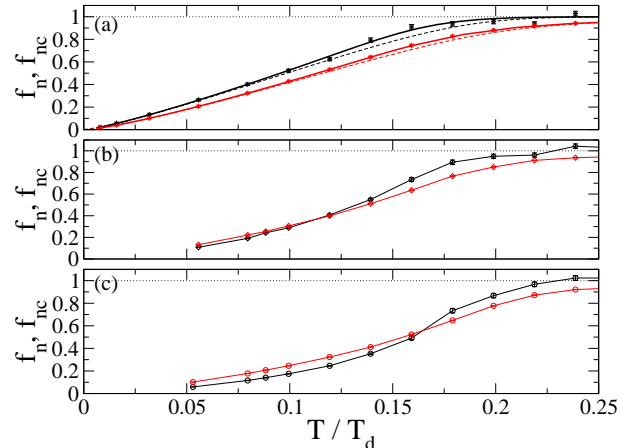


FIG. 5: (Color online) Normal fraction f_n (black) and non-condensed fraction f_{nc} (red) as functions of temperature for a two-dimensional Bose gas with $N = 1000$ particles on a square box of size L with periodic boundary conditions. (a) Ideal Bose gas. (b) Interacting gas with a coupling constant $g_0 = 0.1\hbar^2/m$. (c) Interacting gas with $g_0 = 0.333\hbar^2/m$. Symbols: results of semi-classical simulations on a 64×64 grid with 2000 realizations. Solid lines: in (a) exact result from the canonization procedure (see text); in (b) and (c), a guide to the eye. Dashed lines in (a): the grand canonical predictions. The temperature is in units of the degeneracy temperature T_d such that $k_B T_d = 2\pi\hbar^2 n/m$.

ted in Fig.5a and compared to the Monte Carlo ones. The agreement is remarkable.

2. Density fluctuations

In Fig.6 we plot the temperature dependence of the pair distribution function (33) of the gas evaluated at coincident points $\mathbf{r} = \mathbf{r}'$, i.e. $g^{(2)}(0)$ [49]. In [11] this quantity was related in a classical field model to the notion of a quasi-condensate density in the low temperature superfluid regime, $n_{QC} = n\sqrt{2 - g^{(2)}(0)}$. In the figure, the dependence of $g^{(2)}(0)$ is shown for three values of the interaction strength $mg_0/\hbar^2 = 0, 0.1, 0.333$. In the ideal gas case $g_0 = 0$, the Monte Carlo results are in remarkable agreement with the exact canonical results obtained from the canonization procedure [50]; on the other hand, at low temperatures, when a significant condensed fraction is present, the grand canonical prediction $g^{(2)}(0) = 2$ strongly differs from the canonical results and becomes physically incorrect. Concerning the dependence on the interaction strength g_0 , our simulations confirm the expected trend that an increase of the interaction strength g_0 at a fixed value of the non-condensed fraction corresponds to a strong decrease of the density fluctuations.

Comparing Fig.6 to Fig.5, it is immediate to see that density fluctuations are already significant in the range of

temperatures corresponding to the rapid increase of the normal fraction. This shows that density fluctuations may play an important role in the superfluid transition of a 2D gas [17, 28].

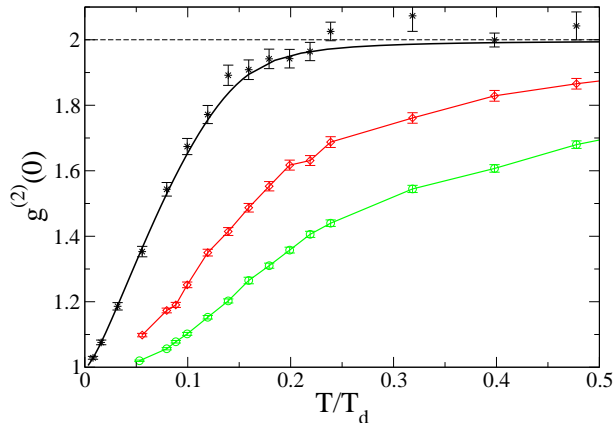


FIG. 6: (Color online) Pair distribution function $g^{(2)}(0)$ as a function of temperature for the same parameters as in Fig.5. Symbols: results of the semi-classical simulations. From top to bottom, the value of the coupling constant increases from $g_0 = 0$ (black stars) to $g_0 = 0.1\hbar^2/m$ (red diamonds) and $0.333\hbar^2/m$ (green circles). Solid lines: for $g_0 = 0$ the exact result from the canonization procedure, for $g_0 > 0$ a guide to the eye. Horizontal dashed line: grand canonical prediction $g^{(2)}(0) = 2$ for the ideal gas. The temperature is in units of the degeneracy temperature T_d such that $k_B T_d = 2\pi\hbar^2 n/m$.

3. Vortex density

In the semi-classical theory, it is straightforward to define a vortex density by looking for the vortices that appear in each stochastic realization of the classical field $\psi(\mathbf{r})$. This is an advantage with respect to e.g. Path Integral Quantum Monte Carlo methods [12].

The field $\psi(\mathbf{r})$ of the semi-classical method, initially defined on a lattice, may be extended to any point of the continuous space by means of the Fourier formula

$$\psi(\mathbf{r}) = \frac{1}{L} \sum_{\mathbf{k}} a_{\mathbf{k}} e^{i\mathbf{k}\cdot\mathbf{r}}, \quad (43)$$

where the $a_{\mathbf{k}}$ are the Fourier components of the field on the lattice. As usual, vortices correspond to nodes in the field ψ with a non-zero circulation; numerically, they can be efficiently and precisely located by calculating the circulation of the phase gradient of the field ψ around plaquettes of much smaller size than the original lattice cell [51].

Numerical results for the mean density of positive charge vortices $n_{v,+}$ as a function of temperature for various interaction strengths are shown in Fig.7a. Thanks

to the periodic boundary conditions, each realization of the field has the same number of positively and negatively charged vortices, which implies $n_{v,-} = n_{v,+}$. For the considered finite size system, there is no qualitative difference between an ideal and an interacting gas: in both cases, the vortex density varies roughly linearly with temperature at high temperature, while it decreases very rapidly at low temperature. Looking at the same data on the logarithmic-reciprocal scale of panel (b), it is easy to observe that the low temperature decrease of $n_{v,+}$ roughly follows an activation law of the form $\propto e^{-\Delta/k_B T}$. A thorough and analytic explanation of this central issue will be given in section III B for the non-interacting $g_0 = 0$ case and in Sec.III C for the general case.

4. Pair distribution function for vortices

As a last observable, it is interesting to look at the pair distribution function for vortices. In analogy with the pair distribution functions for particles in a gas, and restricting for simplicity our attention to the case of opposite charge vortices, this may be defined as

$$G_{v,+ -}^{(2)}(\mathbf{r}) = \langle \rho_{v,+}(\mathbf{0}) \rho_{v,-}(\mathbf{r}) \rangle. \quad (44)$$

For a given realization of the field, $\rho_{v,\pm}(\mathbf{r})$ is here the sum of Dirac deltas $\delta(\mathbf{r} - \mathbf{r}_{v,\pm})$ centered on the locations $\mathbf{r}_{v,\pm}$ of the positive (respectively negative) charge vortices. The angular average of $G_{v,+ -}^{(2)}$ is plotted as a function of the distance r in Fig.8 for different values of the coupling constant g_0 and temperature.

In Fig.8a, a high temperature (but still degenerate) case is considered, where both the normal and the non-condensed fractions are close to unity: a peak appears in all curves at $r = 0$ as well as a plateau at larger vortex separations r . The former is a consequence of the effective attraction among opposite charge vortices, while the latter corresponds to the decorrelated value $G_{v,+ -}^{(2)} \simeq n_{v,+} n_{v,-}$. These numerical results indicate a weak dependence on the interaction strength, and are in good agreement with the known result (not shown) for the ideal gas in the grand canonical ensemble [29, 30, 54].

In Fig.8b, the considered temperatures are low enough to be in the regime where $n_{v,+}$ drops very rapidly with T . For each value of the interaction strength g_0 , the temperature is selected to give a roughly fixed vortex density. A noticeable difference between the ideal and the interacting gas cases appears: the correlations between opposite charge vortices have a much longer range in the ideal gas than in the interacting one.

A more intuitive representation of these issues is given in Fig.9, where the locations of the vortices are shown for some randomly selected Monte Carlo realizations of the field. The high temperature case is considered in (a1) for the ideal gas and in (a2) for the interacting gas. The effect of interactions in the low-temperature regime is visible in panels (b1) and (b2): the difference in behavior

between the ideal (b1) and the interacting (b2) gas cases is apparent, the vortex pairs in the ideal gas being much larger.

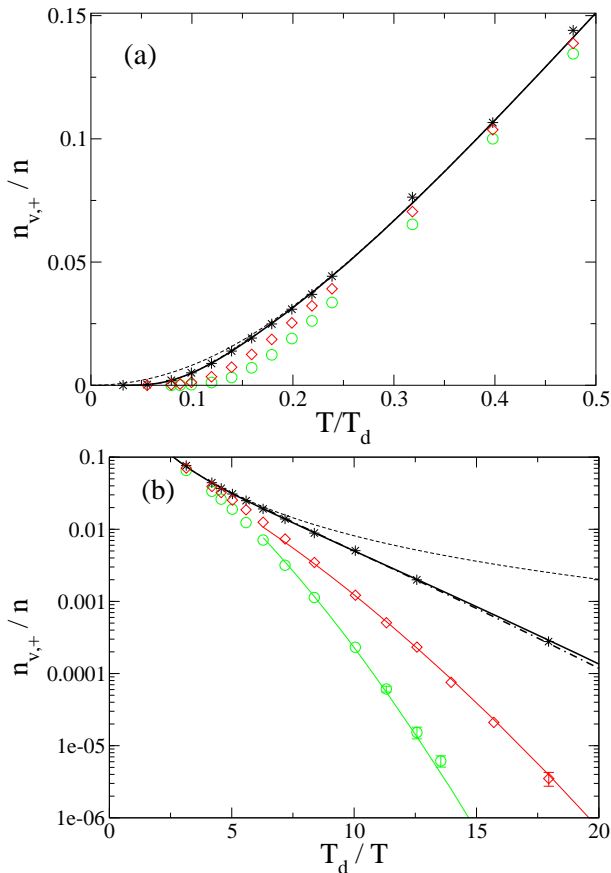


FIG. 7: (Color online) Mean density of positive charge vortices as a function of temperature for various interaction strengths. The parameters have the same values as in Fig.5. (a) Linear scale, (b) logarithmic scale for the vortex density, reciprocal scale for the temperature. Symbols: results of the semi-classical simulation, $g_0 = 0$ (black stars), $g_0 = 0.1\hbar^2/m$ (red diamonds), $g_0 = 0.333\hbar^2/m$ (green circles). Solid lines : the exact canonical result (46) for $g_0 = 0$; prediction of the activation law model of Sec.III C for $g_0 > 0$, $n_{v,+}/n = Ce^{-\Delta(T)/k_B T}$, with the prefactor C taken as a constant and fitted to the data ($C = 0.134$ for $g_0 = 0.1\hbar^2/m$ and $C = 0.3355$ for $g_0 = 0.333\hbar^2/m$). Dashed line: grand canonical result for $g_0 = 0$. Dot-dashed line: Bogoliubov prediction for $g_0 = 0$ for $T/T_d < 0.15$, essentially indistinguishable from the solid line in (a). Note that the circle with the largest value of T_d/T corresponds to $k_B T/n g_0 \simeq 1.4$, which is on the limit of the validity of both the semi-classical field method and of the simple model of section III C calculating Δ .

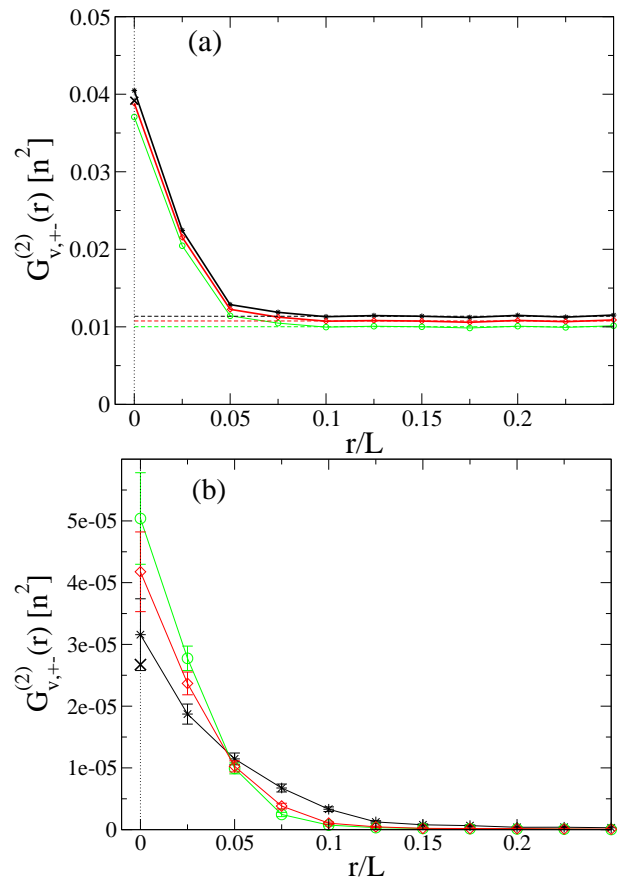


FIG. 8: (Color online) Results of the semi-classical simulations for the angular average $G_{v,+}^{(2)}(r)$ of the pair distribution function for opposite charge vortices as a function of the distance r between the two vortices. The parameters have the same values as in Fig.5. (a) High-temperature, non-Bose condensed regime, temperature $T/T_d = 2.5/(2\pi) \simeq 0.398$, for $m g_0/\hbar^2 = 0$ (black stars), 0.1 (red diamonds), 0.333 (green circles). The solid lines are a guide to the eye. Horizontal dashed lines: square of the mean vortex density $n_{v,+}^2$, showing the decorrelation at long distances. (b) Low temperature, Bose-condensed regime. The temperatures are adjusted to have similar vortex densities for the various values of $g_0 = 0$ (black stars, $T/T_d = 0.35/(2\pi) \simeq 0.056$, leading to $n_{v,+} \simeq 0.28/L^2$), $g_0 = 0.1\hbar^2/m$ (red diamonds, $T/T_d = 0.5/(2\pi) \simeq 0.08$, leading to $n_{v,+} \simeq 0.23/L^2$), $g_0 = 0.333\hbar^2/m$ (green circles, $T/T_d = 0.625/(2\pi) \simeq 0.1$, leading to $n_{v,+} \simeq 0.23/L^2$). The solid lines are a guide to the eye. In both panels (a) and (b), the cross at $r = 0$ gives the exact value of $G_{v,+}^{(2)}$ for the ideal gas, obtained with the canonization procedure. The distance r is in units of L and $G_{v,+}^{(2)}$ is in units of the squared particle density n^2 .

B. The effect of Bose condensation on the vortex density in an ideal gas: Bogoliubov theory

To understand the simulation results for the vortex density in the non-interacting case, a naive approach is

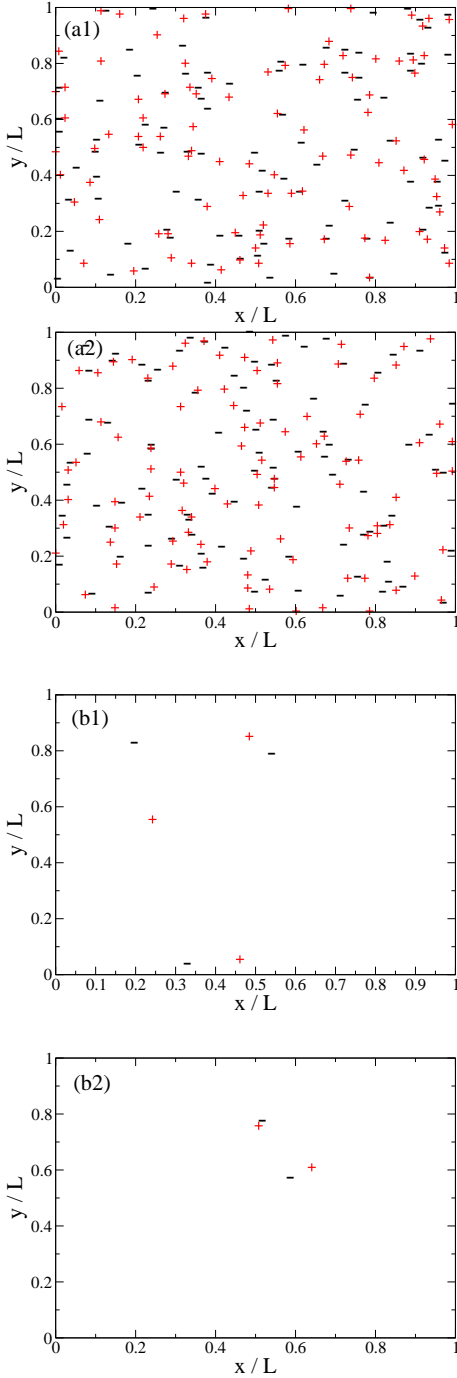


FIG. 9: (Color online) For arbitrary Monte Carlo realizations of the field with vortices, locations of the positive charge vortices (red plus symbols) and negative charge vortices (black minus symbols) in the field. Parameters as in some curves of Fig.8: (a1) $T/T_d = 2.5/(2\pi) \simeq 0.398$ for $g_0 = 0$. (a2) $T/T_d = 2.5/(2\pi) \simeq 0.398$ for $g_0 = 0.333\hbar^2/m$. (b1) $T/T_d = 0.35/(2\pi) \simeq 0.056$ for $g_0 = 0$. (b2) $T/T_d = 0.625/(2\pi) \simeq 0.1$ for $g_0 = 0.333\hbar^2/m$. Note that the realizations shown in (b1) and (b2) are not fully typical since they contain several pairs.

to use the grand canonical ensemble. In this case, the Glauber-P distribution for the field is indeed Gaussian, so that exact analytical predictions can be obtained for the vortex density [29, 30]:

$$(n_{v,+})_{\text{GC}} = \frac{m}{4\pi\hbar^2} \frac{\sum_{\mathbf{k}} E_{\mathbf{k}} n_{\mathbf{k}}}{\sum_{\mathbf{k}} n_{\mathbf{k}}}, \quad (45)$$

where $E_{\mathbf{k}} = \hbar^2 k^2 / 2m$, the mean occupation numbers are given by the Bose formula, $n_{\mathbf{k}} = 1 / \{\exp[\beta(E_{\mathbf{k}} - \mu)] - 1\}$, and the chemical potential μ is adjusted to have the same density of particles as in the canonical ensemble.

This prediction is plotted as a dashed line in Fig.7. While it is able to correctly reproduce the linear behavior of the canonical result in the high temperature regime, it strongly deviates from it at low temperature: the activation law observed in the simulations is then replaced in the grand canonical ensemble by a quadratic dependence on T . As we shall see in what follows, this deviation is due to the presence of a condensate, and is similar to the one predicted in [52] for a rotating two-dimensional ideal Bose gas in the lowest Landau level. Of course, this pathology of the grand canonical ensemble can be eliminated by a canonization procedure for the vortex density, as explained in [52]. We give here only the resulting formula:

$$(n_{v,+})_{\text{C}} = \frac{m}{4\pi\hbar^2} \frac{\int_0^{2\pi} d\theta e^{-i\theta N} B(\theta) \frac{\sum_{\mathbf{k}} E_{\mathbf{k}} \tilde{n}_{\mathbf{k}}(\theta)}{\sum_{\mathbf{k}} \tilde{n}_{\mathbf{k}}(\theta)}}{\int_0^{2\pi} d\theta e^{-i\theta N} B(\theta)}, \quad (46)$$

where the generating function $B(\theta)$ is written as

$$B(\theta) = \prod_{\mathbf{k}} \tilde{n}_{\mathbf{k}}(\theta) \quad (47)$$

in terms of a modified Bose law

$$\tilde{n}_{\mathbf{k}}(\theta) = \frac{1}{e^{\beta(E_{\mathbf{k}} - \mu)} + e^{i\theta}}. \quad (48)$$

As one can see in Fig.7, the predictions of this formula, are in perfect agreement with the simulation results for $g_0 = 0$.

A physical understanding of the strong suppression of vortices in the ideal gas when a condensate is present can be obtained by means of the following approximate treatment based on the Bogoliubov assumption that the fluctuations of the field in the condensate mode are negligible. The 2D classical field ψ can then be expanded as:

$$\psi(\mathbf{r}) = \psi_0 + \sum_{\mathbf{k} \neq 0} a_{\mathbf{k}} \frac{e^{i\mathbf{k} \cdot \mathbf{r}}}{L}, \quad (49)$$

where the condensate amplitude is fixed to the constant value

$$\psi_0 = \left(\frac{\langle N_0 \rangle_{\text{Bog}}}{L^2} \right)^{1/2} = \left(\frac{N - \langle \delta N \rangle_{\text{Bog}}}{L^2} \right)^{1/2}. \quad (50)$$

Here $\langle N_0 \rangle_{\text{Bog}}$ is the mean number of condensate particles in Bogoliubov theory and the mean number of non-condensed particles $\langle \delta N \rangle_{\text{Bog}}$ in Bogoliubov theory is given by

$$\langle \delta N \rangle_{\text{Bog}} = \sum_{\mathbf{k} \neq 0} \frac{1}{e^{\beta E_{\mathbf{k}}} - 1}. \quad (51)$$

Each of the $a_{\mathbf{k}}$'s is a complex random variable with a Gaussian distribution [53]:

$$P_{\mathbf{k}}(\alpha) \propto e^{-|\alpha|^2 (e^{\beta E_{\mathbf{k}}} - 1)}. \quad (52)$$

Since the non-condensed part of the field obeys Gaussian statistics, the calculation of the mean vortex density can be analytically performed,

$$(n_{v,+})_{\text{Bog}} = \frac{m}{4\pi\hbar^2} \frac{\sum_{\mathbf{k} \neq 0} \frac{E_{\mathbf{k}}}{e^{\beta E_{\mathbf{k}}} - 1}}{\langle \delta N \rangle_{\text{Bog}}} e^{-\langle N_0 \rangle_{\text{Bog}} / \langle \delta N \rangle_{\text{Bog}}}. \quad (53)$$

The prediction of this formula is plotted in Fig.7 as a dot-dashed line: the agreement with the exact results is good. It is apparent that the dramatic suppression of the vortices in the presence of a condensate originates from the last factor in Eq.(53), which is indeed exponentially small in the number of condensate particles. One can note that a similar factor is involved in the expression for the probability to have an empty condensate mode in the canonical ensemble. On the other hand, the anomalously large vortex density in the grand canonical ensemble can be explained by the fact that the most probable value for the number of particles in the condensate mode is zero in this ensemble.

Before concluding this section, it is important to remind that (53) is an approximate expression. A first necessary condition for its validity is that a condensate is present, which implies $N \gg \langle \delta N \rangle_{\text{Bog}}$. For a large box $L \gg \lambda_{\text{th}}$ (λ_{th} is here the thermal de Broglie wavelength $\lambda_{\text{th}}^2 = 2\pi\hbar^2/mk_B T$), this condition corresponds to

$$n\lambda_{\text{th}}^2 \gg 2 \log(L/\lambda_{\text{th}}). \quad (54)$$

Another necessary condition for the validity of (53) is that the configurations of the field with vortices are still well described by the Bogoliubov model originally derived for a vortex free field. More precisely, Eq.(50) has to hold also in presence of vortices, e.g. one has to require that the mean number of non-condensed particles *conditioned* to the presence of a vortex, say in $\mathbf{r} = \mathbf{0}$, remains very close to $\langle \delta N \rangle_{\text{Bog}}$. This conditional non-condensed number is defined as

$$\langle \delta N \rangle^{\text{cond}} = \frac{\langle \delta[\psi(\mathbf{r} = 0)] \sum_{\mathbf{k} \neq 0} |a_{\mathbf{k}}|^2 \rangle}{\langle \delta[\psi(\mathbf{r} = 0)] \rangle} \quad (55)$$

where the expectation value is taken over the exact field distribution, δ is the two-dimensional Dirac distribution and the $a_{\mathbf{k}}$'s are the Fourier components of the field. Calculating (55) within Bogoliubov approximation leads to

the validity condition

$$\langle \delta N \rangle_{\text{Bog}}^{\text{cond}} - \langle \delta N \rangle_{\text{Bog}} = \left(2 \frac{\langle N_0 \rangle_{\text{Bog}}}{\langle \delta N \rangle_{\text{Bog}}} - 1 \right) \times \sum_{\mathbf{k} \neq 0} \left(\frac{1}{e^{\beta E_{\mathbf{k}}} - 1} \right)^2 \times \frac{1}{\langle \delta N \rangle_{\text{Bog}}} \ll \langle \delta N \rangle_{\text{Bog}}. \quad (56)$$

In the large box limit $L \gg \lambda_{\text{th}}$, this condition reduces to the simple condition

$$n\lambda_{\text{th}}^2 \ll \frac{4\pi^2}{A} [\log(L/\lambda_{\text{th}})]^3, \quad (57)$$

where the numerical coefficient $A = \sum_{\mathbf{q} \in \mathbb{Z}^{2*}} q^{-4} \simeq 6.0268$. Note that the two conditions (54) and (57) are well compatible in the large box limit $L \gg \lambda_{\text{th}}$, and define a finite validity interval for the Bogoliubov formula (53).

C. General analytical model for the vortex density

In this subsection we provide a physical explanation to the numerical observation that the vortex density follows an approximate activation law at low temperature. This is done by developing a simple and physically transparent model whose predictions turn out to be in good quantitative agreement with the semi-classical simulations presented in section III A, for both the ideal and the interacting cases.

The idea is to look for an approximate field distribution of the form

$$P_{\text{simple}}[\psi] = e^{-\beta U[\psi]} \delta(N - \|\psi\|^2), \quad (58)$$

where $\|\psi\|^2 = dV \sum_{\mathbf{r}} |\psi(\mathbf{r})|^2$, with a suitably chosen energy functional $U[\psi]$. As a temperature independent energy functional (e.g. the Gross-Pitaevskii one (8)) would introduce an unacceptable cut-off dependence [55], we are forced to allow for a temperature dependence of U .

In the ideal gas case, we can reproduce the reasoning of Sec.II C starting from a different representation of the infinite temperature density operator,

$$\rho(\tau = 0) = \int \mathcal{D}\psi \frac{e^{-\|\psi\|^2}}{N!} |N : \psi\rangle \langle N : \psi|, \quad (59)$$

which comes from the projection of the standard over-completeness relation for the Glauber coherent states onto the N -particle subspace. Note that ψ now runs over the whole functional space and is no longer restricted to the unit sphere. The evolution (41) is then applied to each initial Fock state; in the $g_0 = 0$ case, this can be solved analytically. Taking the field ψ at 'time' β rather than at time 0 as integration variable, we can write

$$\rho(\beta) = \int \mathcal{D}\psi P_0[\psi] |N : \psi/\|\psi\|\rangle \langle N : \psi/\|\psi\||, \quad (60)$$

with the field distribution $P_0[\psi]$ equal to

$$P_0[\psi] = e^{-\|\psi\|^2} \frac{\|\psi\|^{2N}}{N!} e^{-\sum_{\mathbf{k}} |a_{\mathbf{k}}|^2 (e^{\beta E_{\mathbf{k}}} - 1)}. \quad (61)$$

$a_{\mathbf{k}}$ is here the Fourier component of the field ψ on the normalized plane wave $e^{i\mathbf{k}\cdot\mathbf{r}}/V^{1/2}$. The $\|\psi\|$ dependent prefactor allows for fluctuations of $\|\psi\|^2$ at most of order $O(N^{1/2})$ around N , which, in the large N limit, is a relatively small quantity as compared to N . By approximating the prefactor with a Dirac delta imposing $\|\psi\|^2 = N$ [56], we finally obtain the desired form (58), with the energy functional

$$U_0[\psi] = \sum_{\mathbf{k}} |a_{\mathbf{k}}|^2 k_B T (e^{\beta E_{\mathbf{k}}} - 1). \quad (62)$$

For the eigenmodes of energy $E_{\mathbf{k}} \ll k_B T$, this energy functional essentially reduces to the non-interacting Gross-Pitaevskii energy functional, while for the eigenmodes of energy $E_{\mathbf{k}} \gg k_B T$ the large value of $e^{\beta E_{\mathbf{k}}}$ strongly reduces the modulus of $a_{\mathbf{k}}$, as required by the Bose law for a quantum field.

This construction can then be heuristically extended to the interacting case. Restricting ourselves to relatively high temperatures $k_B T \gg g_0 n$, we can assume that the modes for which the interaction energy plays a significant role have an energy $\lesssim g_0 n$ and can be treated within a classical field treatment. This amounts to adding the usual interaction term of the Gross-Pitaevskii energy functional [57] to the ideal gas functional (62):

$$U[\psi] = \sum_{\mathbf{k}} |a_{\mathbf{k}}|^2 k_B T (e^{\beta E_{\mathbf{k}}} - 1) + \frac{g_0}{2} \int d^2\mathbf{r} |\psi|^4. \quad (63)$$

As the norm of ψ is fixed to N in (58), the energy functional U can be rewritten in the more convenient form

$$U[\psi] = \frac{N}{\|\psi\|^2} \sum_{\mathbf{k}} |a_{\mathbf{k}}|^2 k_B T (e^{\beta E_{\mathbf{k}}} - 1) + \frac{g_0 N^2}{2 \|\psi\|^4} \int d^2\mathbf{r} |\psi|^4, \quad (64)$$

which is invariant under multiplication of ψ by a global factor, and allows to formally relax the condition $\|\psi\|^2 = N$.

The fact that the formation of vortices at low temperature is an activated process results from the fact that the minimal value of $U[\psi]$ for a field with at least one node is strictly larger than the absolute minimum of $U[\psi]$ (which corresponds to a nodeless ψ). The activation energy $\Delta(T)$ is given by:

$$\Delta(T) \equiv \min_{\psi \text{ with a node}} U[\psi] - \min_{\psi \text{ nodeless}} U[\psi], \quad (65)$$

and its temperature dependence originates from the temperature dependence of the energy functional U . In the regime $k_B T \ll \Delta(T)$, the probability to have the field with at least one node has the activation form:

$$p_{\text{node}} \simeq e^{-\Delta(T)/k_B T} \frac{\int_{\psi \text{ with a node}} \mathcal{D}\psi e^{-\beta(U[\psi]-\Delta)}}{\int_{\psi \text{ nodeless}} \mathcal{D}\psi e^{-\beta U[\psi]}} \quad (66)$$

where the fraction in the right-hand side has an entropic origin and is expected to be a slowly varying function of T .

The general strategy to calculate Δ is what follows. Assuming without loss of generality that the node is in $\mathbf{r} = \mathbf{0}$, the $\mathbf{k} = \mathbf{0}$ Fourier component $a_{\mathbf{0}}$ of the Bose field can be expressed in terms of the other components:

$$a_{\mathbf{0}} = - \sum_{\mathbf{k} \neq \mathbf{0}} a_{\mathbf{k}}. \quad (67)$$

The energy functional $U[\psi]$ is then a function of the $a_{\mathbf{k} \neq \mathbf{0}}$ only and can be minimized without having to impose any further constraint.

The calculation of $\Delta(T)$ is straightforward in the ideal gas case. We have to impose that the first order differential of $U[\psi]$ with respect to the $a_{\mathbf{k}}$'s vanishes, which leads to the condition [58]

$$a_{\mathbf{k}} = a_{\mathbf{0}} \frac{\Delta/N}{\Delta/N - \eta_{\mathbf{k}}}, \quad (68)$$

where $\eta_{\mathbf{k}} = k_B T (e^{\beta E_{\mathbf{k}}} - 1)$. Inserting this equation into (67) gives a closed equation for the activation energy,

$$1 = \sum_{\mathbf{k} \neq \mathbf{0}} \frac{\Delta/N}{\eta_{\mathbf{k}} - \Delta/N}. \quad (69)$$

A graphical reasoning shows that there exists a unique solution in the interval $0 < \Delta/N < \eta_{2\pi/L}$, which is the smallest root of Eq.(69) and thus gives the value of Δ . In the large box limit $L \gg \lambda_{\text{th}}$, one has the analytic expansion:

$$\Delta = \frac{N}{\sum_{\mathbf{k} \neq \mathbf{0}} \eta_{\mathbf{k}}^{-1}} \left[1 - \frac{\sum_{\mathbf{k} \neq \mathbf{0}} \eta_{\mathbf{k}}^{-2}}{(\sum_{\mathbf{k} \neq \mathbf{0}} \eta_{\mathbf{k}}^{-1})^2} + \dots \right], \quad (70)$$

whose leading term reduces to

$$\Delta \simeq \frac{\pi \hbar^2 n}{m \log(L/\lambda_{\text{th}})}. \quad (71)$$

Remarkably, the condition to be in the activation regime $\Delta \gg k_B T$ is equivalent to the condition (54) for Bose condensation, $N \gg \langle \delta N \rangle_{\text{Bog}}$. Note also that the leading term in (70) coincides with the activation part of the Bogoliubov result (53). The successive term gives a correction to Δ which is negligible as compared to $k_B T$ provided that the validity condition (57) for the Bogoliubov theory is satisfied.

In the interacting case, a numerical minimization of $U[\psi]$ in the subspace of the fields with a node in $\mathbf{r} = \mathbf{0}$ is performed with the conjugate gradient method. As an initial guess, a ψ with random complex Fourier coefficients $a_{\mathbf{k} \neq \mathbf{0}}$ is used. We find that the minimizing field ψ_0 has a uniform phase and has a double node in $\mathbf{r} = \mathbf{0}$. This means that ψ_0 may be taken real and corresponds to the superposition of two, oppositely charged vortices located in the origin.

Note that it is possible to reduce the energy U by continuously transforming this field configuration into a nodeless configuration with just a dip in the density at $\mathbf{r} = \mathbf{0}$. On the other hand, a continuous transformation of this field configuration into a configuration with a pair of closely spaced opposite charge vortices corresponds to an increase of the energy U .

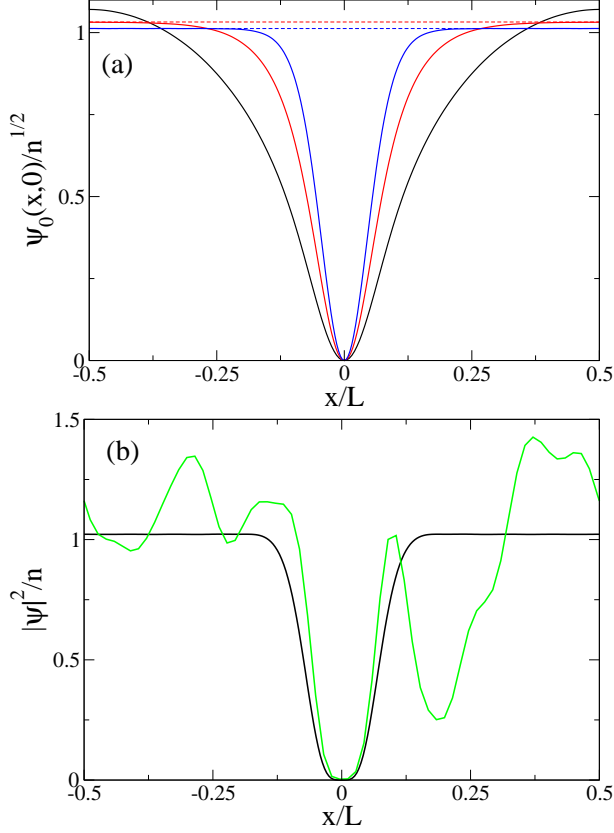


FIG. 10: (Color online) (a) Cut along x -axis of the field ψ_0 minimizing the energy functional $U[\psi]$ over the fields with a node at the origin. Black solid line (the broadest hole): $g_0 = 0$, $T/T_d = 0.35/(2\pi) \simeq 0.056$; red solid line: $g_0 = 0.1\hbar^2/m$, $T/T_d = 0.5/(2\pi) \simeq 0.08$; blue solid line (the narrowest hole): $g_0 = 0.333\hbar^2/m$, $T/T_d = 0.625/(2\pi) \simeq 0.1$. The total number of particles is $N = 1000$. The dashed lines for $g_0 > 0$ correspond to a field value $(\mu/g_0)^{1/2}$, where μ is the Lagrange multiplier defined in Eq.(74). (b) For a semi-classical Monte Carlo realization of the field with a single vortex pair with a small radius, comparison of the density profile of the field (green solid line) with the one of the minimizer ψ_0 of $U[\psi]$ with a node (black solid line). Here $g_0 = 0.333\hbar^2/m$, $T/T_d = 0.5/(2\pi) \simeq 0.08$, the vortex pair diameter is $\simeq 0.03L$ and the origin of the coordinates was redefined to match the location of the vortex pair.

In Fig.10a we show a cut of the field ψ_0 along x axis for the same parameters as in Fig.8b. In Fig.10b we compare the corresponding density profile to the one of a randomly chosen Monte Carlo realization with a small radius vortex pair: there is an acceptable agreement, specially considering the significant density fluctuations in the sim-

ulation result even at the low value of the temperature considered here. It is apparent on Fig.10a that the field ψ_0 has a slowly varying long-distance tail in the ideal gas case, whereas it rapidly reaches its limiting value in the interacting case. This can be understood analytically as follows.

For the ideal gas in the thermodynamic limit, one uses Eqs.(67) and (68), neglecting Δ/N with respect to η_k (for $k \geq 2\pi/L$) and then replacing the sum over \mathbf{k} by an integral, to obtain the approximate expression

$$\psi_0(\mathbf{r}) \simeq a_0 L \frac{\Delta}{N} \int \frac{d^2\mathbf{k}}{(2\pi)^2} \frac{1 - \cos \mathbf{k} \cdot \mathbf{r}}{\eta_k}, \quad (72)$$

which holds for r much smaller than the box size L . In the limit of large $r \gg \lambda_{\text{th}}$, the integral is dominated by the contribution of the low momenta, which results in the functional form

$$\psi_0(\mathbf{r}) \propto \ln(r/\lambda_{\text{th}}). \quad (73)$$

In the interacting case, a sort of generalized Gross-Pitaevskii equation can be derived, expressing the fact that ψ_0 is an extremum of $U[\psi]$ under the constraint that the norm is constant and a node is present in $\mathbf{r} = \mathbf{0}$,

$$\begin{aligned} & \left[k_B T \left(e^{-\beta \hbar^2 \nabla^2 / 2m} - 1 \right) + g_0 |\psi_0|^2 - \mu \right] \psi_0(\mathbf{r}) \\ & = \left(-\mu L a_0 + g_0 \int |\psi_0|^2 \psi_0 \right) \delta(\mathbf{r}). \end{aligned} \quad (74)$$

μ is here the Lagrange multiplier associated to the condition of a constant norm for ψ . Using the numerical fact that ψ_0 is a real function and assuming that at large distance from the origin the laplacian term $\nabla^2 \psi_0$ is negligible, it is easy to see that ψ_0^2 has to converge to the limiting value μ/g_0 . The normalization condition $\|\psi_0\|^2 = N$ then leads to $\mu \simeq g_0 n$ in the large L limit. To see how fast ψ_0 reaches its limiting value, we set $\psi_0(\mathbf{r}) = (\mu/g_0)^{1/2} [1 + \varphi(r)]$ and we linearize the equation in φ ,

$$\left[k_B T \left(e^{-\beta \hbar^2 \nabla^2 / 2m} - 1 \right) + 2\mu \right] \varphi(r) \simeq 0. \quad (75)$$

We heuristically assume that, at large r , φ varies slowly at the scale of the thermal de Broglie wavelength. The first operator in the above equation may then be approximated by the usual kinetic energy operator, so that

$$\left[-\frac{\hbar^2 \nabla^2}{2m} + 2\mu \right] \varphi(r) \simeq 0. \quad (76)$$

The solution is $\varphi(r) \propto K_0(2r/\xi)$ where ξ is the healing length, and $K_0(u)$ is a Bessel function that tends to zero at large u as $e^{-u}/u^{1/2}$. As a consequence, at large r ,

$$\psi_0(\mathbf{r}) = \left(\frac{\mu}{g_0} \right)^{1/2} \left[1 + O\left(e^{-2r/\xi} \right) \right]. \quad (77)$$

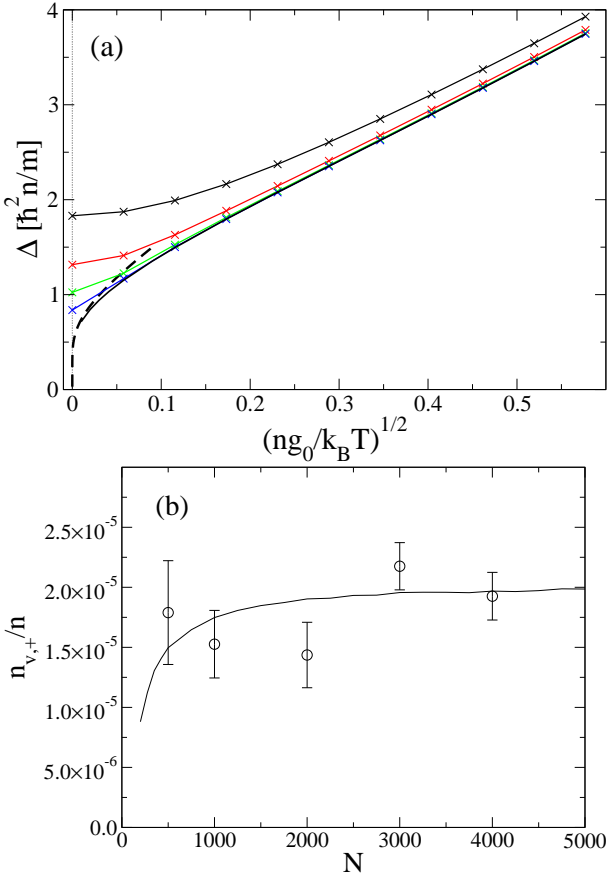


FIG. 11: (Color online) (a) Activation energy $\Delta(T)$ as a function of $(g_0 n/k_B T)^{1/2}$ at a fixed particle density n for increasing system size $L/\lambda_{th} = 6, 12, 24, 48$ (thin solid lines, respectively black, red, green, blue, from top to bottom; the crosses are the actually calculated values and the lines are a guide to the eye). The dashed line is the upper bound Eq.(78) for an infinite system size. The thick solid line is the improved upper bound discussed around Eq.(79), plotted for $(ng_0/k_B T)^{1/2} \geq 0.01$. (b) Vortex density as a function of the total particle number (for increasing system sizes) for fixed values of the density n and the temperature $T = 0.5 T_d/(2\pi) \simeq 0.08 T_d$, and a coupling constant $g_0 = 0.333 \hbar^2/m$. Circles: semi-classical simulations. Solid line: prediction of the activation law $0.44 e^{-\Delta/k_B T}$ where the numerical factor 0.44 was fitted to the data.

Since $k_B T \gg g_0 n$, one indeed finds that, at large r , $\varphi(r)$ varies slowly at the scale of λ_{th} , so that our heuristic assumption is *a posteriori* justified.

This discussion reveals a key difference for the activation energy between the ideal gas and the interacting gas in the thermodynamic limit. While in the ideal gas case the activation energy tends to zero in the thermodynamic limit, in the interacting case it has a non-zero limit. This point is illustrated in Fig.11a, where we plot the activation energy Δ as a function of $(g_0 n/k_B T)^{1/2}$ for increasing system sizes at a fixed particle density n . Away from the origin $g_0 = 0$, a nice convergence towards

a universal curve is obtained, while the dependence of Δ on the system size remains apparent for $g_0 = 0$. A physical interpretation of this fact is that, in the interacting case, the minimizer ψ_0 exponentially converges to a limiting value for $r \gg \xi$, whereas in the ideal gas case it is logarithmically sensitive to the box size L .

As a consequence of a non-zero value for the activation energy in the thermodynamic limit, we expect that the vortex density is an intensive quantity for the interacting gas. This is confirmed by results of Monte Carlo simulations for the vortex density as a function of the system size at fixed density and temperature: note on Fig.11b how the vortex density is remarkably constant in the thermodynamic limit.

As is apparent in Fig.11a, the convergence of the activation energy Δ to its thermodynamic limit value is not uniform in $ng_0/k_B T$ but becomes slower and slower for smaller interaction strength. Analytical results can be obtained for an infinite size system, as detailed in the appendix C: One finds an upper bound on the thermodynamic limit value Δ_∞ of the activation energy,

$$\Delta_\infty \leq \frac{2\pi\hbar^2 n}{m} \frac{1 - 2ng_0/k_B T}{\ln[k_B T/(2ng_0)]}. \quad (78)$$

This explicit upper bound is represented by a dashed line in Fig.11a. It shows that Δ_∞ tends to zero for vanishing interaction strength, which makes a physical link with the ideal gas result Eq.(71) in the thermodynamic limit $L/\lambda_{th} \rightarrow \infty$.

A better upper bound, though requiring some numerics, is obtained by performing a variational calculation, based on the thermodynamic limit of the ansatz

$$\psi(\mathbf{r}) = \mathcal{N} \sum_{\mathbf{k} \neq 0} \frac{1 - \cos(\mathbf{k} \cdot \mathbf{r})}{\exp(E_k/k_B T_{\text{eff}}) - 1 + \alpha}, \quad (79)$$

where \mathcal{N} is a normalisation factor. The two variational parameters are an ‘effective’ temperature T_{eff} and $\alpha \geq 0$. The physical motivation for this ansatz, as well as the way to implement it in the thermodynamic limit, are given in the appendix C. The prediction of this ansatz is shown as a thick solid line in Fig.11a: it is almost indistinguishable (on the figure) from the numerical results for the largest system sizes, except in $g_0 = 0$ where the numerical results suffer from finite size effects.

The success of this ansatz is due to the fact that it reproduces in a fairly accurate way the spatial shape of ψ_0 both at short and long distances: In the limit $ng_0 \ll k_B T$ the energy minimisation leads to $T_{\text{eff}} \simeq T$ and $\alpha \simeq 1.5 ng_0/k_B T$. At distances $r \ll \xi$ one is then allowed to neglect α in the denominator of (79). In this way, one recovers the ideal gas result (73) and, in addition, one obtains the normalization factor which depends on the interaction strength,

$$\psi_0(\mathbf{r}) \sim \frac{2 \ln(r/\lambda_{th})}{\ln(1/\alpha)}. \quad (80)$$

In the large r limit $r \gg \xi$, the ansatz reproduces the exponentially fast convergence of ψ_0 towards its limiting value, Eq.(77), with a decay length differing from the exact one by a numerical factor close to unity, $\simeq 1.15$.

From Eq.(80), it is possible to estimate the half-width at half maximum of the hole in the density profile ψ_0^2 : in the $g_0 \rightarrow 0$ limit, a result growing as $\lambda_{\text{th}} (\xi/\lambda_{\text{th}})^{1/\sqrt{2}}$ is found. This prediction is in good agreement with the numerical results of Fig.11a for $g_0 > 0$ and the largest sample size, $L = 48\lambda_{\text{th}}$.

IV. CONCLUSIONS

In this paper, we have introduced a semi-classical field method for the study of the thermal equilibrium state of an ideal or weakly interacting Bose gas at finite temperature. We have validated the method by verifying that it does not suffer from ultraviolet divergences and it provides quantitatively accurate predictions as long as the temperature is higher than the chemical potential of the gas. The method being based on a probability distribution in the functional space of c-number wavefunctions, it appears as being particularly well suited to the study of thermal vortices, in contrast to standard Quantum Monte Carlo techniques.

As a first application of the method to a system of current experimental interest, we have calculated in this paper the density of thermal vortices in a spatially homogeneous, two-dimensional Bose gas at thermal equilibrium and we have characterized the spatial correlations between the positions of opposite-charged vortices. The numerical results are then used as a starting point to develop simple analytical models and obtain an insight in the physics of the system in the different regimes.

In both the ideal and the interacting cases, in the low temperature limit, the vortex density depends on temperature according to an activation law of the form $\exp(-\Delta/k_B T)$, with an activation energy Δ weakly dependent on temperature. For the ideal gas, Δ is non-zero for a finite size system, because Bose-Einstein condensation takes place in such a system at low enough temperature; for the same reason, Δ depends on the system size and tends logarithmically to zero in the thermodynamic limit. For the interacting gas, Δ has a non-zero value in the thermodynamic limit, reached for a system size larger than the healing length ξ ; this thermodynamic limit value of Δ tends to zero logarithmically in the limit of a vanishing interaction strength.

Finally, we have studied the spatial correlations between the positions of vortices. At high temperatures, no qualitative difference appears between the ideal and the interacting cases. On the other hand, at low temperatures (i.e. in the activation regime), the correlations have a much longer range in the ideal gas, which corresponds to the existence of larger size vortex pairs.

Acknowledgments

We acknowledge the contribution of Bruno Durin and Carlos Lobo in developing a code for locating the vortices at an early stage of this work. We acknowledge useful discussions with Jean Dalibard, Markus Holzmann, Zoran Hadzibabic, and David Hutchinson.

APPENDIX A: QUANTUM AND SEMI-CLASSICAL GLAUBER-P DISTRIBUTIONS FOR A SINGLE BOGOLIUBOV MODE

In this appendix we calculate the exact Glauber-P distribution $P(\gamma)$ and its semi-classical approximation $P_{\text{SC}}(\gamma)$ for the thermal density operator of a single mode Hamiltonian of the form (16).

The imaginary-time evolution of the Glauber-P distribution $P(\gamma)$ is very similar to the one (6) of the full many-body Hamiltonian:

$$\partial_\tau P(\gamma) = -E_1(\gamma) P(\gamma) - \left\{ \partial_\gamma [F_1(\gamma) P(\gamma)] + \frac{\mu}{4} \partial_\gamma^2 P(\gamma) + \text{c.c.} \right\}. \quad (\text{A1})$$

In the (x, y) variables defined as the real and the imaginary parts of the field $\gamma = x + iy$, the mean-field energy $E_1(\gamma)$ and the drift force have the simple form:

$$E_1(\gamma) = (E_k + 2\mu) x^2 + E_k y^2 \quad (\text{A2})$$

$$F_1(\gamma) = -\frac{1}{2} [(E_k + 2\mu) x + iE_k y], \quad (\text{A3})$$

while the diffusion matrix is non-positive definite due to the squeezing terms \hat{c}^2 and $(\hat{c}^\dagger)^2$ in the Hamiltonian.

The analysis of the exact $P(\gamma)$ is most easily done by looking at its Fourier transform, i.e. the normally ordered characteristic function [33]:

$$\chi_P(\xi) = \langle e^{\xi \hat{c}^\dagger} e^{-\xi^* \hat{c}} \rangle, \quad (\text{A4})$$

where the expectation value is taken on the normalized thermal density operator. For a normalized Gaussian density operator originating from the imaginary-time evolution under a quadratic Hamiltonian such as (16), Wick theorem implies that:

$$\chi_P(\xi) = \exp \left[\frac{1}{2} (\xi^2 \langle \hat{c}^\dagger \hat{c}^\dagger \rangle + \xi^{*2} \langle \hat{c} \hat{c} \rangle - 2 |\xi|^2 \langle \hat{c}^\dagger \hat{c} \rangle) \right]. \quad (\text{A5})$$

From the Gaussian structure of $\chi_P(\xi)$, it is immediate to see that the Glauber-P distribution is positive and regular if and only if:

$$\langle \hat{c}^\dagger \hat{c} \rangle > |\langle \hat{c} \hat{c} \rangle|. \quad (\text{A6})$$

Applying this to the Bogoliubov theory provides the condition on the thermal mode occupation:

$$n_k = \frac{1}{e^{\beta \epsilon_k} - 1} > \frac{1}{2} \left[\left(\frac{E_k + 2\mu}{E_k} \right)^{1/2} - 1 \right], \quad (\text{A7})$$

which is plotted in Fig.1.

We now turn to the semi-classical approximation. The solution of the evolution of γ under the drift force, Eq.(11), is a simple scaling transformation:

$$x(\beta) = e^{-(E_k+2\mu)\beta/2} x(0) \quad (\text{A8})$$

$$y(\beta) = e^{-E_k\beta/2} y(0). \quad (\text{A9})$$

An explicit form of the weight $\mathcal{W}(x(0), y(0); \beta)$ is then obtained by inserting the explicit solution (A8-A9) into (12) and integrating it. The result is a Gaussian distribution as a function of $(x(0), y(0))$:

$$\mathcal{W}(\beta) = \exp\{-[(1 - e^{-\beta(E_k+2\mu)}) x(0)^2 + (1 - e^{-\beta E_k}) y(0)^2]\}. \quad (\text{A10})$$

The semi-classical approximation (13) to the (unnormalized) Glauber-P distribution is finally obtained by simply writing (A10) in terms of the final variables $(x(\beta), y(\beta))$ for which $\gamma = x(\beta) + iy(\beta)$. As the Jacobian of the rescaling transformation (A8-A9) is a constant (independent of $x(0)$ and $y(0)$), the result is the Gaussian distribution (17) with the widths given by (20,21).

APPENDIX B: NUMERICAL ALGORITHM IN THE CANONICAL ENSEMBLE

At $\tau = 0$, a wavefunction $\psi(0)$ has to be randomly selected on the unit sphere, and then let evolve until $\tau = \beta = 1/k_B T$ according to (41). This provides the final value $\psi(\beta)$ of the wavefunction to be used in (40). The observables are then computed as averages over the different realizations. As (41) is purely deterministic, this reduces to an averaging over the possible initial wavefunctions $\psi(0)$.

In order to improve the statistical properties of the Monte Carlo code, an importance sampling technique [61] has been implemented in terms of an *a priori* probability distribution $Q[\psi(0)]$. The expectation value of a generic operator \hat{O} is rewritten as:

$$\langle \hat{O} \rangle = \frac{1}{\mathcal{Z}} \int_{\|\psi\|=1} \mathcal{D}\psi(0) Q[\psi(0)] \frac{\langle N : \psi(\beta) | \hat{O} | N : \psi(\beta) \rangle}{Q[\psi(0)]}, \quad (\text{B1})$$

where \mathcal{Z} is the normalisation factor. If the distribution of the initial wavefunction $\psi(0)$ is sampled with a probability law proportional to $Q[\psi(0)]$, one is left with the average of a quantity

$$\frac{\langle N : \psi(\beta) | \hat{O} | N : \psi(\beta) \rangle}{Q[\psi(0)]} \quad (\text{B2})$$

which can be made flatter by means of a clever choice of $Q[\psi(0)]$. This provides significant improvement to the statistical properties of the Monte Carlo code. In our simulations the form

$$Q[\psi(0)] = \langle N : \psi(\beta) | N : \psi(\beta) \rangle = \|\psi(\beta)\|^{2N} \quad (\text{B3})$$

is used for the *a priori* probability distribution $Q[\psi(0)]$. This choice was motivated by the requirement that the integrand (B2) be flat at least for the calculation of the partition function, i.e. the trace of the density operator. In the numerical code, the sampling of $Q[\psi(0)]$ is performed by means of a standard Metropolis algorithm based on rotations in the single-particle Hilbert space, similarly to what was done in [62].

Another way of sampling $Q[\psi(0)]$ (not used in this work) could be the following. At each step of the Metropolis algorithm, a multiplication of the amplitude of $\psi(0)$ on one (randomly chosen) mode of the system by a random complex number $z = e^\lambda e^{i\alpha}$ is proposed. The phase α is uniformly distributed in $[0, 2\pi[$ and the logarithm λ of the modulus has an even probability distribution over the real axis. Subsequently one renormalizes $\psi(0)$. One can check that this procedure preserves the detailed balance condition required by the Metropolis algorithm, since the probability distributions of z and of $1/z$ coincide.

APPENDIX C: UPPER BOUND ON THE ACTIVATION ENERGY Δ IN THE THERMODYNAMIC LIMIT

In this appendix we derive an upper bound on the thermodynamic limit value of the activation energy Eq.(65) for an interacting gas $g_0 > 0$.

To take the thermodynamic limit in the energy functional $U[\psi]$, we set

$$\psi(\mathbf{r}) = \mathcal{N} f(\mathbf{r}) \quad (\text{C1})$$

where $f(0) = 0$ and $f(\mathbf{r})$ reaches rapidly unity at large r/ξ . The normalization factor is given by

$$|\mathcal{N}|^2 \left[L^2 + \int_{L^2} (|f|^2 - 1) \right] = N, \quad (\text{C2})$$

where we have subtracted and added one to $|f|^2$. As $|f|^2 - 1$ is an exponentially narrow function of r for $L \rightarrow \infty$, the integral in Eq.(C2) rapidly converges in the thermodynamic limit, so that we get the expansion

$$|\mathcal{N}|^2 = n \left[1 - \frac{1}{L^2} \int (|f|^2 - 1) + O(1/L^4) \right] \quad (\text{C3})$$

where the integral is now over the whole plane. This allows to calculate the deviation $\delta U_\infty[f]$ between $U[\psi]$ and the nodeless ground state energy $N^2 g_0 / 2L^2$ in the thermodynamic limit, as a functional of f . For $U_0[\psi]$ the knowledge of the leading order term of the normalization factor \mathcal{N} in (C3) is sufficient, whereas for the interaction energy the $1/L^2$ correction is required. We obtain

$$\delta U_\infty[f] = nk_B T \int f^* \left[e^{-\beta \hbar^2 \nabla^2 / 2m} - 1 \right] f + \frac{g_0 n^2}{2} \int (|f|^2 - 1)^2. \quad (\text{C4})$$

To easily obtain an upper bound on the thermodynamic limit value Δ_∞ of the activation energy, we restrict to the class \mathcal{C} of real and isotropic functions f such that $0 \leq f(\mathbf{r}) \leq 1$ for all \mathbf{r} . Then $(|f|^2 - 1)^2 = (1 - f)^2(1 + f)^2 \leq 4(1 - f)^2$, so that

$$\Delta_\infty \leq W[f] = nk_B T \int f^* \left[e^{-\beta \hbar^2 \nabla^2 / 2m} - 1 \right] f + 2g_0 n^2 \int (1 - f)^2, \quad \forall f \in \mathcal{C}. \quad (\text{C5})$$

It remains to minimize the energy functional $W[f]$ over the class \mathcal{C} , which is conveniently done in the Fourier space representation

$$f(\mathbf{r}) = \frac{\int \frac{d^2 \mathbf{k}}{(2\pi)^2} u(\mathbf{k})(1 - \cos \mathbf{k} \cdot \mathbf{r})}{\int \frac{d^2 \mathbf{k}}{(2\pi)^2} u(\mathbf{k})}, \quad (\text{C6})$$

a writing which ensures that $f(0) = 0$ and $f \rightarrow 1$ at infinity for a smooth (real) function $u(\mathbf{k})$. This representation leads to

$$W[f] = n \frac{\int \frac{d^2 \mathbf{k}}{(2\pi)^2} (\eta_k + 2ng_0) u(\mathbf{k})^2}{\left[\int \frac{d^2 \mathbf{k}}{(2\pi)^2} u(\mathbf{k}) \right]^2}. \quad (\text{C7})$$

Imposing that the functional derivative of this expression with respect to u vanishes leads to the choice

$$u_m(\mathbf{k}) = \frac{1}{\eta_k + 2ng_0}. \quad (\text{C8})$$

One can check, at least for $k_B T > 2ng_0$, that the corresponding function $f_m(r)$ indeed takes values between 0 and 1 only, so that it belongs to the class \mathcal{C} and it is the minimizer of $W[f]$ [59]. This results in the upper bound [60]

$$\Delta_\infty \leq W[f_m] = \frac{2\pi \hbar^2 n}{m} \frac{1 - 2ng_0/k_B T}{\ln[k_B T/(2ng_0)]}. \quad (\text{C9})$$

The variational ansatz Eq.(79) is deduced from Eq.(C8) by replacing the physical parameters T and $2ng_0$ by two variational parameters T_{eff} and $\alpha k_B T_{\text{eff}}$.

-
- [1] Yu. Kagan, B. V. Svistunov, and G. V. Shlyapnikov, Sov. Phys. JETP **75**, 387 (1992); Yu. Kagan and B. V. Svistunov, Phys. Rev. Lett. **79**, 3331 (1997); N. G. Berloff and B. V. Svistunov, Phys. Rev. A **66**, 013603 (2002).
- [2] K. Damle, S. N. Majumdar and S. Sachdev, Phys. Rev. A **54**, 5037 (1996).
- [3] M.J. Davis, S.A. Morgan and K. Burnett, Phys. Rev. Lett. **87**, 160402 (2001).
- [4] K. Góral, M. Gajda, K. Rzążewski, Opt. Express **8**, 92 (2001); D. Kadio, M. Gajda and K. Rzążewski, Phys. Rev. A **72**, 013607 (2005).
- [5] G. Baym, J.-P. Blaizot, M. Holzmann, F. Laloë and D. Vautherin, Phys. Rev. Lett. **83**, 1703 (1999).
- [6] P. Arnold and G. Moore, Phys. Rev. Lett. **87**, 120401 (2001); V. A. Kashurnikov, N. V. Prokof'ev, and B. V. Svistunov, Phys. Rev. Lett. **87**, 120402 (2001).
- [7] D.J. Scalapino, M. Sears, R.A. Ferrell, Phys. Rev. B **6**, 3409 (1972).
- [8] Y. Castin, R. Dum, E. Mandonnet, A. Minguzzi, I. Carusotto, Journal of Modern Optics **47**, 2671 (2000).
- [9] T. P. Simula, M. D. Lee, and D. A. W. Hutchinson, Phil. Mag. Lett. **85**, 395 (2005); T. P. Simula and P. B. Blakie, Phys. Rev. Lett. **96**, 020404 (2006).
- [10] N. Prokof'ev, O. Ruebenacker, and B. Svistunov, Phys. Rev. Lett. **87**, 270402 (2001).
- [11] N. Prokof'ev and B. Svistunov, Phys. Rev. A **66**, 043608 (2002).
- [12] D. M. Ceperley, Rev. Mod. Phys. **67**, 279 (1995).
- [13] M. Boninsegni, N. V. Prokof'ev, and B. V. Svistunov, Phys. Rev. E **74**, 036701 (2006).
- [14] W. Krauth, Phys. Rev. Lett. **77**, 3695 (1996); M. Holzmann, W. Krauth, and M. Naraschewski, Phys. Rev. A **59**, 2956 (1999); M. Holzmann and W. Krauth, Phys. Rev. Lett. **83**, 2687 (1999).
- [15] P. Grüter, D. Ceperley, and F. Laloë, Phys. Rev. Lett. **79**, 3549 (1997).
- [16] I. Carusotto and Y. Castin, Phys. Rev. Lett. **90**, 030401 (2003).
- [17] A. I. Safonov, S. A. Vasilyev, I. S. Yasnikov, I. I. Lakashevich, and S. Jaakkola, Phys. Rev. Lett. **81**, 4545 (1998).
- [18] A. Görlitz, J. M. Vogels, A. E. Leanhardt, C. Raman, T. L. Gustavson, J. R. Abo-Shaeer, A. P. Chikkatur, S. Gupta, S. Inouye, T. Rosenband, and W. Ketterle, Phys. Rev. Lett. **87**, 130402 (2001); V. Schweikhard, I. Coddington, P. Engels, V. Mogendorff, and E. A. Cornell, Phys. Rev. Lett. **92**, 040404 (2004); D. Rychtarik, B. Engeser, H.-C. Nägerl, and R. Grimm, Phys. Rev. Lett. **92**, 173003 (2004); N. L. Smith, W. H. Heathcote, G. Hechenblaikner, E. Nugent, and C. J. Foot, J. Phys. B **38**, 223 (2005); C. Orzel, A. K. Tuchman, M. L. Fenselau, M. Yasuda, and M. Kasevich, Science **291**, 2386 (2001); S. Burger, F. S. Cataliotti, C. Fort, P. Maddaloni, F. Minardi and M. Inguscio, Europhys. Lett. **57**, 1 (2002); Z. Hadzibabic, S. Stock, B. Battelier, V. Bretin, and J. Dalibard, Phys. Rev. Lett. **93**, 180403 (2004).
- [19] S. Stock, Z. Hadzibabic, B. Battelier, M. Cheneau, and J. Dalibard, Phys. Rev. Lett. **95**, 190403 (2005).
- [20] Z. Hadzibabic, P. Krüger, M. Cheneau, B. Battelier, and J. Dalibard, Nature **441**, 1118 (2006).
- [21] V. Schweikhard, S. Tung, and E. A. Cornell, preprint arXiv:0704.0289 [cond-mat.mes-hall].
- [22] V. L. Berezinskii, Zh. Eksp. Teor. Fiz. **61**, 1144 (1971) [Sov. Phys. JETP **34**, 610 (1972)]; J. M. Kosterlitz and D. J. Thouless, J. Phys. C **5**, L124 (1972); J. M. Kosterlitz and D. J. Thouless, J. Phys. C **6**, 1181 (1973); J. M. Kosterlitz, J. Phys. C **7**, 1047 (1974).

- [23] P. Minnhagen, Rev. Mod. Phys. **59**, 1001 (1987).
- [24] M. Holzmann, G. Baym, J.-P. Blaizot, F. Laloë, PNAS **104**, 1476 (2007).
- [25] M. Le Bellac, *Quantum and statistical field theory* (Clarendon Press, Oxford, 1991).
- [26] A. Smerzi, P. Sodano, and A. Trombettoni, J. Phys. B **37**, S265 (2004).
- [27] A. Trombettoni, A. Smerzi, P. Sodano, New J. Phys. **7**, 57 (2005).
- [28] Yu. Kagan, V. A. Kashurnikov, A. V. Krasavin, N. V. Prokof'ev, and B. V. Svistunov, Phys. Rev. A **61**, 043608 (2000).
- [29] B. I. Halperin, Les Houches lecture series, eds. R. Balian, M. Kléman and J.-P. Poirier, Vol.35, p. 813 (North-Holland, Amsterdam, 1981).
- [30] M. V. Berry and M. R. Dennis, Proc. R. Soc. Lond. A **456**, 2059 (2000).
- [31] R. J. Glauber, Phys. Rev. **131**, 2766 (1963); R. J. Glauber, Phys. Rev. Lett. **10**, 84 (1963).
- [32] D. F. Walls and G. J. Milburn, *Quantum Optics* (Springer-Verlag, Berlin, 1994).
- [33] C. Gardiner and P. Zoller, *Quantum Noise* (Springer, Heidelberg, 2004).
- [34] Here \sim is taken in the strict mathematical sense, $f \sim g$ if $\lim f/g = 1$.
- [35] A. J. Leggett, Rev. Mod. Phys. **71**, S318 (1999).
- [36] N. V. Prokof'ev and B. V. Svistunov, Phys. Rev. B **61**, 11282 (2000).
- [37] Note that the value of f_n predicted by the present Bogoliubov theory neglects the possibility that the gas populates quasi-condensate states with a non-zero momentum, that is with non-zero winding numbers along x or y . In the thermodynamic limit, this is not a problem in three dimensions. On the other hand, inclusion of non-zero winding numbers leads to significant corrections in two dimensions [36], and dramatically changes the value of f_n in one dimension [36, 38].
- [38] I. Carusotto and Y. Castin, Comptes Rendus Physique **5**, 107 (2004).
- [39] I. Carusotto, Y. Castin, J. Dalibard, Phys. Rev. A **63**, 23606 (2001).
- [40] D. S. Petrov, D. M. Gangardt, and G. Shlyapnikov, Lecture notes of Les Houches school on *low dimensional quantum gases*, J. Phys. IV France, **116**, 5 (2004).
- [41] This is correct provided that the typical energies per particle (the chemical potential or the thermal energy scale $k_B T$) do not assume exponentially small values $\lesssim \hbar\omega_z e^{-\sqrt{2\pi}a_{ho}/a_{3D}}$.
- [42] Y. Castin, R. Dum, Eur. Phys. J. D **7**, 399-412 (1999).
- [43] Note that the numerical results reported here have been obtained for a finite-size system, whose physics is in many aspects very different from the one in the thermodynamic limit. In this latter case, the non-condensed fraction is in fact one for all $T > 0$, while the normal fraction tends to zero for T tending to zero and shows a finite jump at the Kosterlitz-Thouless transition temperature [22]. In the finite systems, the non-condensed fraction is reduced and the BKT universal jump smeared out. A discussion of the interplay between the Kosterlitz-Thouless transition and Bose-Einstein condensation in finite-size 2D systems can be found in [27, 44].
- [44] S. T. Bramwell and P. C. W. Holdsworth, Phys. Rev. B **49**, 8811 (1994).
- [45] M. Wilkens, C. Weiss, Opt. Express **1**, 272 (1997).
- [46] C. Herzog, M. Olshanii, Phys. Rev. A **55**, 3254 (1997).
- [47] M. Holthaus and E. Kalinowski, Ann. Phys., NY **276**, 321 (1999) and references therein.
- [48] The (unnormalized) density operator ρ_N in the canonical ensemble is obtained from the grand canonical one ρ_{GC} by projecting this latter onto the subspace with N atoms. The projector on this subspace \mathcal{P}_N can be written in the form: $\mathcal{P}_N = \int_0^{2\pi} d\theta e^{i\theta(\hat{N}-N)}/(2\pi)$, where \hat{N} is the particle number operator. The density operator in the canonical ensemble is then written as the N th Fourier harmonic of the grand canonical one ρ_{GC} with a complex chemical potential $\tilde{\mu} = \mu + i\theta/\beta$:
- $$\rho_N = \int_0^{2\pi} \frac{d\theta}{2\pi} e^{-\beta H} e^{(\beta\mu+i\theta)\hat{N}} e^{-i\theta N}.$$
- All expectation values can be calculated from this form by means of a numerical integration over θ .
- [49] In a fully quantum lattice model, $g^{(2)}(0)$ in 2D depends on microscopic aspects of the model, i.e. the lattice spacing; this clearly appears in the so-called quantum term in the Bogoliubov theory [63]. But $g^{(2)}(0)$ as predicted by the semi-classical theory cannot capture this microscopic aspect and rather has to be interpreted as an extrapolation from the macroscopic length scales such as the healing length ξ or the thermal de Broglie wavelength λ_{th} down to zero, as is apparent in Fig.4 for the Bogoliubov gas.
- [50] Note that, in the thermodynamic limit, the ideal gas is not Bose condensed at any $T > 0$, so that $g^{(2)}(0) = 2$ (matter wave Hanbury-Brown and Twiss effect [64]). On the other hand, $g^{(2)}(0) - 1$ would be strongly reduced in an interacting 2D gas [17, 28] at low temperature even in the absence of a condensate, the so-called quasi-condensate phenomenon [63, 65, 66, 67, 68, 69].
- [51] In practice, each side of a plaquette is divided in many sub-intervals of length dl . Over each of them, the field is assumed to vary linearly with the position. The coefficients of this linear expansion are deduced from the value of ψ and of its derivative at the center of the sub-interval. This linear expansion is then used to calculate analytically the integral of the gradient of the phase of ψ over each sub-interval, and the contributions of the different sub-intervals are then summed up. It is easy to see why this procedure is much more efficient than assuming a linear variation of the phase along each sub-interval: while the phase shows rapid variations in the vicinity of a vortex core, the variation of the field ψ is always smooth.
- [52] Y. Castin, Z. Hadzibabic, S. Stock, J. Dalibard, S. Stringari, Phys. Rev. Lett. **96**, 040405 (2006).
- [53] Formally, one uses for the non-condensed modes $a_{\mathbf{k}} (\mathbf{k} \neq \mathbf{0})$ a grand canonical Glauber-P distribution with a chemical potential $\mu = 0$. This procedure is justified by observing that the condensate mode can be treated as a reservoir of chemical potential $E_0 = 0$.
- [54] It is interesting to remind that in the grand canonical ensemble, a simple formula relates [29, 30] the charge-weighted vortex pair distribution function
- $$G_{v,Q}^{(2)}(\mathbf{r}) = 2[G_{v,++}^{(2)}(\mathbf{r}) - G_{v,-}^{(2)}(\mathbf{r})]$$
- $$= \langle [\rho_{v,+}(\mathbf{0}) - \rho_{v,-}(\mathbf{0})][\rho_{v,+}(\mathbf{r}) - \rho_{v,-}(\mathbf{r})] \rangle$$
- to the one-body correlation function of the atomic gas $g^{(1)}(\mathbf{r} - \mathbf{r}') = \langle \hat{\Psi}^\dagger(\mathbf{r}')\hat{\Psi}(\mathbf{r}) \rangle/n$: in the thermodynamic

limit,

$$G_{v,Q}^{(2)}(r) = \frac{1}{4\pi^2 r} \frac{d}{dr} \left(\frac{[dg^{(1)}/dr(r)]^2}{1 - [g^{(1)}(r)]^2} \right).$$

- [55] Anticipating on further reasonings, one can show for the Gross-Pitaevskii energy functional in the absence of cutoff that the activation energy Δ defined in Eq.(65) is always zero in the thermodynamic limit, even for the interacting gas. This results e.g. from the insertion in Eq.(C4) of a variational ansatz $f(r)$ obtained by setting $u(\mathbf{k}) = e^{-k^2\epsilon}/(1+k^2)$ in Eq.(C6), and by taking the limit $\epsilon \rightarrow 0$.
- [56] One can test this approximation, in the interacting case, using the fact that the reasoning in [57] leads to the functional form $P[\psi] = \|\psi\|^{2N} e^{-\|\psi\|^2 F[\psi/\|\psi\|]}/N!$, and introducing $\int dN' \delta[N' - \|\psi\|^2]$ inside the functional integral over ψ , where N' is an intermediate variable. Then the same reasoning as the one exposed in the text finds an activation energy $\Delta_{\text{bey}} = \Delta/(1 + \beta g_0 n/2)$. Since we are in the limit $ng_0 \ll k_B T$ and Δ varies essentially linearly in $(ng_0/k_B T)^{1/2}$, see Fig.11a, we consider this correction to be beyond the accuracy of the simple model and we disregard it.
- [57] A more systematic derivation of this form can be obtained starting from Eq.(41). First, one treats the interaction terms to first order in time dependent perturbation theory (here for imaginary time). Then, the first order correction is simplified by means of a classical field approximation. Calculation of the weight $\exp[-\|\psi(0)\|^2]$ as a function of $\psi(\beta)$ finally leads to the energy functional U .
- [58] This derivation assumes that $\Delta/N \neq \eta_k$ for all $\mathbf{k} \neq \mathbf{0}$ in the reciprocal lattice. Actually, there exist other solutions $\Delta/N = \eta_{\mathbf{q}}$, where \mathbf{q} is $2\pi/L$ times a non-zero two-dimensional vector with integer components. However, they correspond to higher values of the energy functional and therefore are not relevant to the present discussion.
- [59] Expanding $u_m(\mathbf{k})$ in powers of $\exp(-\beta\hbar^2 k^2/2m)$, one obtains the series expansion $1 - f_m(r) = B \sum_{n \geq 0} (1 - \alpha)^n e^{-R^2/[2(n+1)]}/(n+1)$ with $\alpha = 2\beta n g_0$, $B = (1 - \alpha)/\ln(1/\alpha)$ and $R^2 = r^2 m k_B T/\hbar^2$.
- [60] Let us assume that the minimizer f_0 of $\delta U_\infty[f]$ is a real and increasing function of the distance r to the node location, as suggested by the numerical calculations for a finite size system, so that the function f_0 belongs to the class \mathcal{C} . Then $(1 - f_0^2)^2 \geq (1 - f_0)^2$ so that $\Delta_\infty \geq W'[f_0]$, where the energy functional W' is deduced from W by replacing $2ng_0$ by $ng_0/2$. Since $W'[f_0] \geq \min_{f \in \mathcal{C}} W'[f]$, one finds a lower bound $\Delta_\infty \geq \frac{2\pi\hbar^2 n}{m} \frac{1 - ng_0/2k_B T}{\ln[2k_B T/(ng_0)]}$.
- [61] W. H. Press, S. A. Teukolsky, W. T. Vetterling, and B. P. Flannery, *Numerical Recipes* (Cambridge University Press, Cambridge, 1988).
- [62] Y. Castin, I. Carusotto, *Opt. Commun.* **243**, 81 (2004).
- [63] C. Mora and Y. Castin, *Phys. Rev. A* **67**, 053615 (2003).
- [64] M. Yasuda, F. Shimizu, *Phys. Rev. Lett.* **77**, 3090 (1996); M. Schellekens, R. Hoppeler, A. Perrin, J. Viana Gomes, D. Boiron, A. Aspect, C. I. Westbrook, *Science* **310**, 648 (2005).
- [65] V. N. Popov, *Functional Integrals in Quantum Field Theory and Statistical Physics* (Reidel, Dordrecht, 1983).
- [66] Yu. Kagan, B.V. Svistunov, and G.V. Shlyapnikov, *Sov. Phys. JETP* **66**, 314 (1987).
- [67] U. Al Khawaja, J. O. Andersen, N. P. Proukakis, and H. T. C. Stoof, *Phys. Rev. A* **66**, 013615 (2002).
- [68] S. Dettmer, D. Hellweg, P. Ryytty, J. J. Arlt, W. Ertmer, K. Sengstock, D. S. Petrov, and G. V. Shlyapnikov, *Phys. Rev. Lett.* **87**, 160406 (2001); D. Hellweg, L. Cacciapuoti, M. Kottke, T. Schulte, K. Sengstock, W. Ertmer, and J. J. Arlt, *Phys. Rev. Lett.* **91**, 010406 (2003).
- [69] S. Richard, F. Gerbier, J. H. Thywissen, M. Hugbart, P. Bouyer, and A. Aspect, *Phys. Rev. Lett.* **91**, 010405 (2003).